Elsevier Editorial System(tm) for Neuropharmacology

Manuscript Draft

Manuscript Number: NEUROPHARM-D-18-00432

Title: Oleoylethanolamide restores alcohol-induced inhibition of neuronal proliferation and microglial activity in striatum

Article Type: Research Paper

Keywords: alcohol; PPARα; microglia; neurogenesis; locomotion; striatum

Corresponding Author: Dr. Juan Suarez, Ph. D.

Corresponding Author's Institution: IBIMA-Hospital Regional Universitario de Málaga

First Author: Patricia Rivera, PhD

Order of Authors: Patricia Rivera, PhD; Daniel Silva-Peña, PhD student; Eduardo Blanco, PhD; Antonio Vargas, Lab technician; Sergio Arrabal, PhD; Antonia Serrano, PhD; Francisco J Pavón, PhD; Laura Bindila, PhD; Beat Lutz, PhD; Fernando Rodriguez de Fonseca, PhD; Juan Suarez, Ph. D.

Abstract: Previous findings demonstrate a homeostatic role for oleoylethanolamide (OEA) signaling in the ethanol-related neuroinflammation and behavior. However, extensive research is still required in order to unveil the effects of OEA on a number of neurobiological functions such as adult neurogenesis, cell survival and resident neuroimmunity that become notably altered by alcohol. Daily consumption of ethanol (10%) for 2 weeks (6.3□1.1 g/kg/day during last 5 days) caused hypolocomotor activity in rats. This effect appears to rely on central signaling mechanisms given that alcohol increased the OEA levels, the gene expression of OEA-synthesizing enzyme Nape-pld and the number of PPARα-immunoreactive neurons in the striatum. Ethanol-related neurobiological alterations such as a reduction in the number of microglial cells expressing iNOS (a cytokine-inducible immune defense) and in adult neural stem/progenitor cell (NSPC) proliferation (phospho-H3 and BrdU) and maturation (BrdU/β3-tubulin), as well as an increase in damage cell activity (FosB) and apoptosis (cleaved caspase 3) were also observed in the rat striatum. Pharmacological administration of OEA (10 mg/kg) for 5 days during ethanol exposure exacerbated ethanol-induced hypolocomotion and cell apoptosis in the striatum. Interestingly, OEA abrogated the impaired effects of ethanol on PPARα+ cell population and NSPC proliferation and maturation. OEA also decreased astrocyte activation (vimentin) and increased microglial activation (Iba-1, iNOS) in the striatum. These results suggest that OEA-PPARα signaling modulates glial activation, cell apoptosis and NSPC proliferation and maturation in response to striatal-specific neurobiological alterations induced by prolonged ethanol intake in rats.

HIGHLIGHTS

Oleoylethanolamide (OEA) role in the ethanol-related neuroinflammation and behavior

OEA exacerbated ethanol-induced hypolocomotion and cell apoptosis in rat striatum

OEA abrogated the impaired effects of ethanol on NSPC proliferation and maturation

OEA decreased astrocyte activation and increased microglial activation in striatum

OEA responses to striatal-specific neurobiological alterations induced by ethanol

TITLE PAGE

OLEOYLETHANOLAMIDE RESTORES ALCOHOL-INDUCED INHIBITION OF NEURONAL PROLIFERATION AND MICROGLIAL ACTIVITY IN STRIATUM

Running title: OEA in ethanol impairment of neurogenesis

Patricia Rivera[1], Daniel Silva[2], Eduardo Blanco[3], Antonio Vargas[2], Sergio Arrabal[2], Antonia Serrano[2], Francisco Javier Pavón[2], Laura Bindila[4], Beat Lutz[4], Fernando Rodríguez de Fonseca[2,*], Juan Suárez[2,*]

[1]Department of Endocrinology, Fundación Investigación Biomédica del Hospital Infantil Universitario Niño Jesús, Madrid, Spain. [2]Instituto de Investigación Biomédica de Málaga (IBIMA), UGC Salud Mental, Universidad de Málaga, Hospital Universitario Regional de Málaga, Málaga, Spain. [3]Departament de Pedagogia i Psicologia. Facultat d'Educació, Psicologia i Treball Social. Universitat de Lleida, Lleida, Spain. [4]Institute of Physiological Chemistry, University Medical Center of the Johannes Gutenberg-University of Mainz, and German Resilience Center (DRZ), Mainz, Germany.

***Address for correspondence:**

Juan Suárez, e-mail: juan.suarez@ibima.eu

Fernando Rodríguez de Fonseca, e-mail: fernando.rodrigiez@ibima.eu

Laboratorio de Investigación. IBIMA. Hospital Universitario Regional de Málaga. Avenida Carlos Haya 82, 29010 Málaga, Spain. Tel/fax number: +34952614012.

Abbreviations

AEA, anandamide or *N*-arachidonoylethanolamide; BrdU, 5-bromo-2'-deoxyuridine; Cnr1, cannabinoid type-1 receptor; Faah; fatty acid amide hydrolase; GFAP, glial fibrillary acidic protein; γGT, gamma-glutamyl transferase; GOT, glutamic-oxaloacetic transaminase; GPT, glutamic-pyruvic transaminase; Iba-1 (Aif-1), ionized calcium-binding adapter molecule 1 (allograft inflammatory factor 1); lv, lateral ventricle; Nape-pld; n-acyl phosphatidylethanolamine phospholipase D; OEA, oleoylethanolamide; P-H3, phospho-histone 3; Pparα, peroxisome proliferator-activated receptor alpha; Str, striatum; SVZ, subventricular zone of the lateral ventricles.

ABSTRACT

Previous findings demonstrate a homeostatic role for oleoylethanolamide (OEA) signaling in the ethanol-related neuroinflammation and behavior. However, extensive research is still required in order to unveil the effects of OEA on a number of neurobiological functions such as adult neurogenesis, cell survival and resident neuroimmunity that become notably altered by alcohol. Daily consumption of ethanol (10%) for 2 weeks (6.3±1.1 g/kg/day during last 5 days) caused hypolocomotor activity in rats. This effect appears to rely on central signaling mechanisms given that alcohol increased the OEA levels, the gene expression of OEA-synthesizing enzyme *Nape-pld* and the number of PPARα-immunoreactive neurons in the striatum. Ethanol-related neurobiological alterations such as a reduction in the number of microglial cells expressing iNOS (a cytokine-inducible immune defense) and in adult neural stem/progenitor cell (NSPC) proliferation (phospho-H3 and BrdU) and maturation (BrdU/β3-tubulin), as well as an increase in damage cell activity (FosB) and apoptosis (cleaved caspase 3) were also observed in the rat striatum. Pharmacological administration of OEA (10 mg/kg) for 5 days during ethanol exposure exacerbated ethanol-induced hypolocomotion and cell apoptosis in the striatum. Interestingly, OEA abrogated the impaired effects of ethanol on PPARα+ cell population and NSPC proliferation and maturation. OEA also decreased astrocyte activation (vimentin) and increased microglial activation (Iba-1, iNOS) in the striatum. These results suggest that OEA-PPARα signaling modulates glial activation, cell apoptosis and NSPC proliferation and maturation in response to striatal-specific neurobiological alterations induced by prolonged ethanol intake in rats.

Key words: Alcohol; PPARα; microglia; neurogenesis; locomotion; striatum.

1. INTRODUCTION

The satiety factor oleoylethanolamide (OEA), a structural analogue of the *N*-acylethanolamine (NAE) arachidonoyl ethanolamide (AEA or anandamide), is a bioactive lipid mediator that exerts a number of pharmacological effects on lipid and glucose metabolism, energy expenditure and satiety/motivated responses to dietary fat, through the highly potent activation of the peroxisome proliferator-activated receptor-alpha (PPARα) (Guzmán et al., 2004; Piomelli, 2013; Suárez et al., 2014; Bilbao et al., 2016). The intestine is able to produce OEA upon the input of fat-containing food, a process that activates peripheral sensory systems (vagus nerve), informs to central integrative networks (solitary tract nucleus and hypothalamus) and releases gut peptides into blood in order to regulate energy expenditure (Fu et al., 2011; Serrano et al., 2011). Moreover, growing evidence indicates that OEA serves as a hedonic homeostatic signal in motivated and cognitive processes through the reward and limbic systems in the brain (Campolongo et al., 2009; Rivera et al., 2014), involving food selection (Tellez et al., 2013), dopaminergic responses associated with nicotine-independent mechanism (Mascia et al., 2011) and alcohol-seeking behavior (Bilbao et al., 2016).

A recent study of our group has identified a relevant role of OEA as a homeostatic signal that influences physiological adaptations to alcohol exposure (Bilbao et al., 2016). Alcohol administration triggers OEA production that, in turn, regulates behavioral effects such as motivational response to alcohol and withdrawal symptoms after cessation of alcohol consumption. As a confirmation, it was found that the administration of OEA (5 and 20 mg/kg) and other PPARα agonists (gemfibrozil, Wy 14643, tesaglitazar, and fenofibrate) reduced alcohol intake and self-administration, an effect that depends on PPARα activation (Barson et al., 2009; Ferguson et al., 2014; Bilbao et al., 2016). OEA mobilization following acute alcohol exposure was first observed in the jejunum and nucleus accumbens (Bilbao et al., 2016). Peripherally, alcohol-enhanced sympathetic activity could be responsible for OEA

mobilization in the intestine and in metabolically-relevant organs such as adipose tissue (LoVerme et al., 2006; Fu et al., 2011). Centrally, alcohol may trigger receptor-dependent OEA activation through the NAPE-PLD pathway (Stella and Piomelli, 2001; Spanagel, 2009). A rapid response of the nucleus accumbens to alcohol may be related to the recruitment of either catecholaminergic, cholinergic and/or glutamatergic neurons (Spanagel, 2009). Moreover, as it was previously described for fats and high-caloric foods (Piomelli, 2013), our hypothesis suggests that the satiety factor OEA is also able to modulate motivational responses to alcohol. In this regard, OEA and other PPARα agonists decreased cue-induced reinstatement of alcohol consumption (Bilbao et al., 2016). This relevant result implies that OEA is capable of controlling contextual memories associated with alcohol relapse. In addition, alcohol withdrawal symptoms are supported by the decrease in OEA levels and its adaptive nature as a homeostatic signal (Bilbao et al., 2016). Interestingly, OEA injection at the beginning of withdrawal (when OEA levels are dropping) produced a lower severity of the withdrawal symptoms. These results support previous clinical studies suggesting that OEA levels are altered in alcohol-dependence during abstinence and might be a potential marker for predicting length of alcohol abstinence (García-Marchena et al., 2017). Human genetic reports also described an association between alcohol use disorders and polymorphisms/mutation of the gene encoding the NAE-hydrolyzing enzyme fatty acid amide hydrolase (FAAH) (Sipe et al., 2002).

The endogenous lipid mediators NAEs share common biosynthetic and degradative pathways but not receptor targets (i.e. AEA on the cannabinoid CB1 and CB2 receptors; OEA on PPARα) (Overton et al., 2006; Pertwee, 2008; Ueda et al., 2010; Di Marzo et al., 2011). The NAE signaling systems can be targeted by drugs of abuse (Orio et al., 2013) and, in turn, may mediate neuroprotective effects on alcohol-induced neurodegeneration and cognitive deficits triggered by neuronal cell death and loss of neurogenesis (Nixon and Crews, 2004; Rivera et

al., 2015b). Consequently, alcoholics show significant volume loss in cortical and subcortical brain structures that includes both gray and white matter shrinkage (Crews and Nixon, 2009). In this regards, NAEs may be of interest as they can act on the neuronal stem cells proliferation (Stella, 2010; Katona and Freund, 2012; Galve-Roperh et al., 2013; Bandiera et al., 2014; Rivera et al., 2015b). However, one of the major concerns that have been raised against the use of CB1 receptor agonists arises from results showing that these compounds may increase the intake of drugs of abuse, especially alcohol (Colombo et al., 2005). An alternative to pharmacological cannabinoid activation could be the selective inhibition of FAAH, the primary enzyme responsible for the degradation of AEA, as it does not increase alcohol abuse risk and reduces anxiety associated to alcohol withdrawal (Cippitelli et al., 2008). However, the inhibition of FAAH did not promote adult neurogenesis in alcoholic rats (Rivera et al., 2015b), despite its known effects on neural proliferation in culture and healthy rodent (Aguado, et al., 2005; Goncalves et al., 2008; Rivera et al., 2015a), as well as neuroprotection from brain injury (Fowler et al., 2010).

Because PPARα stimulation might be of potential interest for alcohol dependence (Ferguson et al., 2014; Bilbao et al., 2016), a promising therapy to potentiate central mechanisms leading to neuroprotective and anti-inflammatory effects might be the direct administration of OEA binding to PPARα (Anton et al., 2016). However, at present, it is unclear the neurobiological mechanisms underlying the homeostatic role of OEA-PPARα signaling in the ethanol-related neurodegeneration and behavior such as adult neurogenesis, cell survival and resident neuroimmune cells. To shed light on these questions, the present study was designed to investigate the pharmacological effects of the repeated administration (5 days) of OEA (10 mg/kg), contrasted with those of AEA (10 mg/kg), on astrogliosis (GFAP, vimentin) and microgliosis (Iba-1, iNOS), as well as cell proliferation (phospho-H3, BrdU), maturation (BrdU/β3-tubulin) and apoptosis (cleaved caspase-3) in the striatum and its neurogenic zone,

the subventricular zone of the lateral ventricles (SVZ), of the adult rats with a daily consumption of alcohol (10%) in diet for two weeks.

2. MATERIALS AND METHODS

2.1. Ethics Statement

The protocols for animal care and use were approved by the Ethics and Research Committee at the Hospital Universitario Regional de Málaga and Universidad de Málaga. All experimental animal procedures were carried out in strict accordance with the European Communities directive 86/609/ECC (24 November 1986) and Spanish legislation (BOE 252/34367-91, 2005) regulating animal research. All efforts were made to minimize animal suffering and to reduce the number of animals used.

2.2. Animals

Male Wistar rats (approximately 250 g, 10–12 weeks old; Charles Rivers, Barcelona, Spain) were housed individually in cages maintained in standard conditions (Centro de Experimentación Animal, Universidad de Málaga) at 20 ± 2 ºC room temperature, 40 ± 5% relative humidity and a 12-h light/dark cycle with dawn/dusk effect. Water and standard rodent chow (Prolab RMH 2500, 2.9 kcal/g) were available *ad libitum*, unless otherwise indicated for specific experimental procedures.

2.3. Alcoholic diet habituation

Seventy-two animals were daily weighed, handled for 10 minutes and habituated to injection procedures (holding and pseudo-injection) during one week before the experimentation in order to minimize stress effects. To habituate the animals to feeding procedures, rats were first food-deprived to 95% of their free-feeding weight and then they were allowed *ad libitum*

access to a complete and balanced chocolate-flavored liquid food (0.97 kcal/mL; Glucerna SR, Abbott Laboratories, Madrid, Spain) until a stable rate of feeding was reached (~50 mL/day, up to 2-3 days). Then, the rats were divided into two groups (*n*=36) and fed with the chocolate-flavored liquid diet supplemented with 11% (*v/v*) ethanol 96º (alcoholic liquid diet) or 14.7% (*w/v*) sucrose (sucrose liquid diet) (Serrano et al., 2012). Both alcoholic and sucrose liquid diets were formulated to contain the same calories (1.4 kcal/mL). Thus, the same volume of ethanol liquid diet consumed *ad libitum* was given the next day to the rats fed with the sucrose liquid diet. The rats were maintained under a controlled-isocaloric *per* feeding period until a stable rate of alcoholic feeding was reached (~30 mL/day, up to one week). In any case, standard rodent chow was not given, but water was available *ad libitum*, during the experimentation. Caloric intake and body weight were periodically monitored.

2.4. Administration of OEA and AEA

After alcoholic diet habituation, the rats were fed *ad libitum* with both liquid diets (ethanol or sucrose) and treated with the endogenous PPARα and GPR55 receptor agonist OEA (oleoylethanolamide; cat. no. 1484, Tocris, Abingdon, UK) and the endogenous cannabinoid and TRPV1 receptor agonist AEA (anandamide; cat. no. 1339, Tocris). Drugs were dissolved in a vehicle containing 33% (*v/v*) DMSO in sterile 0.9% NaCl solution, just before each experiment, and were intraperitoneally (i.p.) injected in a final volume of 1 mL/kg of body weight. The optimal dose at which treatment would be more effective in neuroprotection, as described previously (Piomelli et al., 2006; Galán-Rodríguez et al., 2009), was selected for the present study. Thus, OEA and AEA were repeatedly administrated at a dose of 10 mg/kg body weight, for 5 consecutive days at intervals of 24 hours (08:00 a.m.). The animals were sacrificed 2 hours after the last injection of the drugs. Finally, we obtained six experimental groups depending on the diet and treatment (*n*=12): vehicle-treated sucrose-fed group, AEA-

treated sucrose-fed group, OEA-treated sucrose-fed group, vehicle-treated ethanol-fed group, AEA-treated ethanol-fed group and OEA-treated ethanol-fed group.

2.5. BrdU administration

5´-bromo-2´-deoxyuridine (BrdU; cat. no. B5002, Sigma, St. Louis, MO, USA) was dissolved at 15 mg⁄mL in sterile 0.9% NaCl solution. During the *ad libitum* feeding period, BrdU was i.p. administrated at a dose of 50 mg/kg of body weight, twice per day at intervals of 10 hours (08:00, 18:00 h), for 4 consecutive days (Rivera et al., 2015b).

2.6. Open field test

For this behavioral protocol, we used a four square Open Field (OF) (L50 × W50 × H50 cm) mazes during treatment (Panlab, Barcelona, Spain). Arenas were uniformly illuminated with light intensities of 50 lux at the centers of the arenas. The apparatuses were cleaned between sessions with 70% ethanol and then dried. Behavioral tests were carried out between 8:00 and 15:00. Each animal was treated and, 30 minutes later, placed individually in the center of each arena, and the locomotor activity was recorded with a video tracking system (Smart®, Panlab). The testing orders of the treatment groups were counterbalanced to avoid confounding effects of the time of the day at which the animals were tested. Locomotor activity was assessed by measuring the distance traveled (cm) for three time bins of 5 minutes each one.

2.7. Sample collection

Prior to sacrifice, all animals were anaesthetized (sodium pentobarbital, 50 mg/kg body weight, i.p.) two hours after the last dose of treatment in a room separate from the other experimental animals. The blood samples were transcardially collected into tubes containing

EDTA-2Na (1 mg/mL blood) and centrifuged (1600 *g* for 10 min, 4ºC). The plasma samples were then frozen and stored at -80ºC for biochemical and liquid chromatography–multiple reaction monitoring (LC-MRM) analyses.

The first batch of animals (*n* = 6/group) were sacrificed by decapitation and their brains were collected, snap-frozen and stored at −80°C. These brains were then prepared on dry ice to obtain sections of 1 mm thick by using razor blades and a rat brain slicer matrix. The striatum were precisely removed from 2.20 to −0.26 mm of Bregma levels (Paxinos and Watson, 2007) with fine surgical instruments. Brain samples were weighed and stored at −80°C until they were used for RT-qPCR and LC-MRM analysis. The second batch of animals (*n* = 6/group) were transcardially perfused with 4% formaldehyde in 0.1 M phosphate buffer (PB) and the brains were dissected out and kept in the same fixative solution overnight at 4ºC. The brains were then cut into 30-µm-thick coronal sections by using a sliding microtome (Leica VT1000S) and divided in 12 parallel series. Sections were stored at 4ºC in PB with 0.002% (*w*/*v*) sodium azide until they were used for immunostaining.

2.8. *N*-acylethanolamine quantification

The quantitative analysis of OEA and AEA in plasma followed the protocols previously published (Lomazzo et al., 2014; Bindila and Lutz, 2016) with a brief modification. After resuspension of endocannabinoid extract in 50 µL (1:1, ACN:H_20), sample aliquots were prepared by diluting 1:5 in (1:1 v/v, ACN:H_20) prior to injection in the LC/MRM. Twenty µL of the aliquots were injected into the LC/MRM. The brain and plasma endocannabinoid concentrations were normalized to tissue weight and to plasma volume, respectively.

2.9. Ethanol concentration and hepatic enzyme activity in blood

The blood ethanol concentration (BEC) was determined using the alcohol oxidase method with an AM1 Alcohol Analyzer (Analox Instrument, London, UK). The activity of the hepatic enzymes gamma-glutamyl transpeptidase (γGT), glutamate pyruvate transaminase (GPT) and glutamic oxaloacetic transaminase (GOT) were analyzed using commercial kits according to the manufacturer´s instructions in a Hitachi 737 Automatic Analyzer (Hitachi Ltd., Tokyo, Japan). A calibration curve and internal controls were included in each assay.

2.10. RNA isolation and RT-qPCR analysis

We performed real-time PCR (TaqMan, ThermoFisher Scientific, Waltham, MA, USA) as was described previously (Rivera et al., 2015a) using specific sets of primer probes (*Cnr1*: Rn02758689_s1, Amplicon length: 92; *Pparα*: Rn00566193_m1, Amplicon length: 98; *Nape-pld*: Rn01786262_m1, Amplicon length: 71; *Faah*: Rn00577086_m1, Amplicon length: 63; *Actb*: Rn00667869_m1, Amplicon length: 91; ThermoFisher Scientific). Briefly, the striati were homogenized on ice and the RNA was extracted following Trizol® method according to the manufacture's instruction (Gibco BRL Life Technologies, Baltimore, MD, USA). The RNA samples were isolated with RNAeasy minelute cleanup-kit including digestion with DNase I column (Qiagen, Hilden, Germany). After reverse transcript reaction from 1 μg of RNA, quantitative real-time reverse transcription polymerase chain reaction (qPCR) was performed in a CFX96TM Real-Time PCR Detection System (Bio-Rad, Hercules, CA, USA) and the FAM dye label format for the TaqMan® Gene Expression Assays (ThermoFisher Scientific). Melting curve analysis was performed to ensure that only a single product was amplified. After analyzing several control genes, values obtained from the brain samples were normalized in relation to β-actin (*Actb*) levels.

2.11. Immunohistochemistry

Free-floating coronal sections (*n*= 6-7) from one of the 12 parallel series obtained from each rat striatum were selected from 2.20 to −0.26 mm of Bregma levels (Paxinos and Watson, 2007) to perform each immunolabeling. For immunohistochemistry, sections were incubated overnight in the following diluted primary antibody at 4°C: mouse anti-glial fibrillaric acidic protein (GFAP) (1:500; cat. no. G3893, Sigma), mouse anti-vimentin (1:500; cat no. V6630, Sigma), rabbit anti-Iba-1 (1:1000; cat. no. 019-19741, Wako, Neuss, Germany), rabbit anti-iNOS (1:500, ThermoFisher, cat no. PA1-036), rabbit anti-FosB (1:2500; cat. no. sc-48, Santa Cruz Biotechnology, Santa Cruz, CA, USA), rabbit anti-cleaved caspase-3 (1:500; cat. no. 9661, Cell Signaling, Leiden, The Netherlands), rabbit anti-phospho-histone H3 (Ser10) (2 μg/mL; cat. no. 06-570, Merck, Madrid, Spain), and mouse anti-BrdU (1:2000; cat. no. G3G4, Hybridoma Bank, Iowa City, IA, USA) (Rivera et al., 2013).

The following day the sections were incubated in the respective secondary antibody for 90 minutes: biotinylated goat anti-mouse IgG (1:500; cat. no. B7264, Sigma) or biotinylated donkey anti-rabbit IgG (1:500; cat. no. RPN1004, Amersham, Little Chalfont, England). The sections were then incubated in ExtrAvidin peroxidase (Sigma) diluted 1:2000 in darkness at room temperature for 1 hour. Finally, immunoreactivity was revealed with 0.05% diaminobenzidine (DAB; Sigma), 0.05% nickel ammonium sulfate and 0.03% H_2O_2 in PBS.

2.12. Immunofluorescence

The following antibodies were used: mouse anti-PPARα (1:200; cat. no. 20R-PR21, Fitzgerald, Acton, MA, USA), rabbit anti-cleaved caspase-3 (1:500; cat. no. 9661, Cell Signaling), mouse anti-Iba-1 (1:500; cat. no. MABN92, Merck), mouse anti-GFAP (1:500; cat. no. G3893, Sigma), rat anti-BrdU (1:2000; cat. no. OBT0030G, Accurate Chemical and Scientific, Westbury, NY, USA), and mouse anti-β3 tubulin (1:5000; Promega, Madison, WI,

USA). For double immunofluorescence, sections were incubated overnight at 4°C with a cocktail of the primary antibodies and then with the correspondent secondary antibodies: donkey anti-rat IgG (H+L) labeled with Alexa Fluor® 488 (1:1000; cat. no. A21208, Molecular Probes, Invitrogen, Paisley, UK), donkey anti-mouse IgG (H+L) labeled with Alexa Fluor® 594 (1:1000; cat. no. A21203, Molecular Probes), and donkey anti-rabbit IgG labeled with Cy3 bis-NHS ester (1:300; cat. no. 711-166-152, Jackson ImmunoResearch).

2.13. Cell counting

Positive (+) immunoreactive and immunofluorescent nuclei and cells that came into focus were manually counted. Representative counting frames from sections with immunoreactivity were evaluated using a standard optical microscope with the 40× objective (Nikon Instruments Europe B.V., Amstelveen, The Netherlands) coupled to the NIS-Elements Imaging Software 3.00 (Nikon). For immunofluorescent cell counting, the sections were visualized with a confocal laser (spectral) scanning microscope (Leica TCS NT; Leica Microsystems) equipped with a 561 nm DPM laser (argon 30%) and a 40× objective (HCX PL APO CS 40.0x1.25 OIL UV). The emission filter settings were 500–550 nm for PMT2 (green) and 610–700 nm for PMT3 (red). Depending on the level of zoom used in each image, the XY voxel size was from 100 to 77 nm, approximately. Settings of light and brightness/contrast were adjusted by using the Leica LAS AF Lite imaging software. Phospho-H3+ and BrdU+ nucleus counts were performed in the subventricular zone (SVZ) of the lateral ventricles, while GFAP, Iba-1, iNOS, FosB, cleaved caspase-3 and PPARα+ cell counts were carried out in the whole striatum. Overall, quantification was expressed as the average number of cells per area (mm^2) for each experimental group.

2.14. Statistical analysis

Statistical analysis of the results was performed using the computer program GraphPad Prism version 5.04 (GraphPad Software Inc., San Diego, CA, USA). Data were represented as the mean + s.e.m. for at least six determinations per experimental group. Kolmogorov-Smirnov normality tests indicated that all data followed a Gaussian distribution (P>0.1), so we selected a parametric statistical test. Statistical analysis was performed using one-way ANOVA and two-way ANOVA with the two factors being diet or treatment and time, followed by Bonferroni *post hoc* test for multiple comparisons, or Student's *t* test when appropriate. P<0.05 was considered to be significant.

3. RESULTS

3.1. Ethanol consumption

Rats were habituated to a controlled-isocaloric pair-feeding period of sucrose and alcohol diets for 10 days (**Fig. 1A**). During the habituation period, daily consumption of ethanol (10%) in diet reached up to 12.5 ± 1.4 g of ethanol/kg body weight/day. Then, all rats were exposed *ad libitum* to the diets for 6 days. During the *ad libitum* feeding period, daily consumption of ethanol in diet reached an average of 6.3±1.1 g/kg/day. We observed an effect of alcohol ($F_{1,60}$= 1104.42, P< 0.0001) and time ($F_{5,60}$= 204.81, P< 0.0001) on diet consumption, and an interaction between factors ($F_{5,60}$= 97.58, P< 0.0001). The main results indicated that the *ad libitum* consumption of the alcoholic diet, measured as cumulative intake, was lower than that of the sucrose liquid diet from the day 11 onward (day 11, **P<0.01; day 12 on, ***P<0.001) (**Fig. 1B**).

3.2. Effect of ethanol consumption on locomotor activity

We investigated the impact of the ethanol consumption on the locomotor activity (distance travelled for three time bins of 5 minutes each one) by using an Open Field paradigm. We

observed an effect of alcohol ($F_{1,10}$= 13.22, P= 0.01) and time ($F_{2,20}$= 14.12, P= 0.001) on the distance covered for 15 minutes. The main results indicated that rats exposed to alcoholic diet showed a lower distance travelled in the Open Field compared to that of the sucrose group over the 3 time bins of 5 minutes each (*P<0.05) (**Fig. 1C**).

3.3. Effects of ethanol consumption on hepatic enzyme activity in plasma

To evaluate the alcohol-associated toxicity we measured the blood ethanol concentration (BEC) and the activity of the hepatic enzymes gamma-glutamyl transpeptidase (γGT), glutamate pyruvate transaminase (GPT) and glutamic oxaloacetic transaminase (GOT) in plasma. No difference in BEC was found between rats fed with sucrose and alcoholic diet; probably due to a clearance effect during the time spent between the last alcohol intake and the BEC analysis (**Fig. 1D**). However, rats exposed to alcoholic diet showed higher GPT/GOT ratio and γGT plasma levels that those of the sucrose group (*P<0.05) suggesting hepatic toxicity induced by chronic alcohol consumption (**Fig. 1D**).

3.4. Effect of ethanol consumption on the *N*-acylethanolamine levels in plasma and brain

We analyzed the levels of the *N*-acylethanolamines (NAE) OEA and AEA in the plasma (**Fig. 1D**) and the brain regions striatum, hippocampus and hypothalamus (**Fig. 1E**) of rats exposed to sucrose and ethanol. Alcoholic diet induced an increase in the plasma levels of AEA (**P<0.01), but not OEA (**Fig. 1D**). However, both OEA and AEA levels were specifically augmented in the striatum (*P<0.05), but not in the hippocampus and hypothalamus, of rats exposed to alcoholic diet (**Fig. 1E**).

3.5. Effects of ethanol consumption on the mRNA levels of the NAE-metabolizing enzymes and NEA receptors in the striatum

As we found alterations of OEA and AEA levels in the striatum, we analyzed the gene expression of the main NAE-related machinery (*Nape-pld* and *Faah*) and receptors (*Cnr1* and *Pparα*). We observed an increase in the mRNA levels of *Nape-pld* in the striatum of ethanol-exposed rats compared with those of sucrose group (**P*<0.05) (**Fig. 1F**). No changes were found in the striatal gene expression of *Cnr1*, *Pparα* and *Faah*.

3.6. Effect of OEA and AEA on ethanol consumption

OEA and AEA were pharmacologically administered (10 mg/kg) during 5 days and the dietary sucrose or ethanol consumption was evaluated (**Fig. 2A**). Our results indicated an effect of OEA on sucrose diet consumption ($F_{1,50}$= 31.89, *P*< 0.0001), but not ethanol diet consumption. However, we found AEA effects on both sucrose ($F_{1,50}$= 350.13, *P*< 0.0001) and ethanol ($F_{1,50}$= 9.91, *P*= 0.002) diet consumption. Time effects were also observed on both sucrose and ethanol diet consumption of rats treated with OEA and AEA for 5 days ($F_{4,50}$> 15.01, *P*< 0.0001). Interaction between treatment (OEA and AEA) and time was found in rats exposed to sucrose diet ($F_{4,50}$> 8.6, *P*< 0.0001), but not in rats exposed to ethanol diet. Post-hoc analysis indicated that OEA induced an increase in sucrose diet intake on the third and fourth day of treatment (****P*<0.001) (**Fig. 2B**). AEA also induced an increase in sucrose diet intake from the third day onwards (****P*<0.001).

3.7. Effect of OEA and AEA on locomotor activity

We investigated the impact of OEA and AEA in the locomotor activity of rats exposed to ethanol in diet (**Fig. 2D-F**). Rats exposed to sucrose or ethanol in diet and treated with OEA or AEA exhibited a lower distance covered in the Open Field compared to those of the respective vehicle-treated group (sucrose: */***P*<0.05/0.01; ethanol: $^{\#}P$<0.05) (**Fig. 2E**). The OEA-induced decrease in the locomotor activity was exacerbated in rats exposed to ethanol

diet compared to that of the OEA-treated sucrose group ($^{\$}P<0.05$). However, no difference in locomotor activity between rats exposed to sucrose and ethanol diet was found when they were treated with AEA (**Fig. 2E**).

Regarding the alcoholic diet groups, OEA administration induced a decrease in the distance covered during the first 10 minutes of the Open Field test ($^{\#}P<0.05$) (**Fig. 2E**), while AEA treatment only produced a decrease in the distance travelled during the first 5 minutes ($^{\#}P<0.05$) (**Fig. 2F**). The influence of OEA and AEA on the locomotor activity disappear during the last 5 minutes of test.

3.8. Effects of OEA and AEA on hepatic enzyme activity and NAE levels in plasma

To evaluate the treatment effect on ethanol-associated toxicity, we analyzed the activity of the hepatic enzymes γGT, GPT and GOT in the plasma of rats exposed to the alcoholic diet. Our results indicated that OEA administration specifically decreased the GPT/GOT ratio in rats exposed to ethanol ($^{\#}P<0.05$) (**Fig. 2G**). Neither OEA or AEA modified the plasma activity of γGT. The levels of AEA and OEA remained high in plasma at the moment of sacrifice, 2 hours after the last administration, in AEA-treated rats and OEA-treated rats, respectively ($^{\#}P<0.05$) (**Fig. 2H**). Interestingly, we also observed an increase in the plasma levels of AEA in OEA-treated rats exposed to the alcoholic diet ($^{\#}P<0.05$) (**Fig. 2H**). However, AEA-treated rats exposed to ethanol did not exhibited significant changes in the plasma levels of OEA.

3.9. Effect of OEA and AEA on gliosis in the striatum of ethanol-exposed rats

To investigate the impact of OEA and AEA on astroglial and microglial activity in the striatum of ethanol-exposed rats, we evaluated the number of immunoreactive cells for GFAP, Iba-1 and iNOS, as well as vimentin immunoreactivity by densitometry (**Fig. 3**). Regarding astrogliosis, no ethanol effects were found on the number of GFAP+ cells and vimentin

immunoreactivity (**Fig. 3A-J**). Regarding microgliosis, we didn't observe changes in the number of Iba1+ cells, but we detected a decrease in the number of iNOS+ cells in the striatum of ethanol-exposed rats (*P<0.05) (**Fig. 3K-T**). The striatum of the rats exposed to an alcoholic diet and treated with OEA or AEA showed higher number of GFAP+ and Iba-1+ cells compared to that of the ethanol-vehicle group ($^{\#\#/\#\#\#}P$<0.01/0.001) (**Fig. 3A,K**). In contrast, OEA induced a decrease in the striatal levels of vimentin immunoreactvity ($^{\#}P$<0.05) (**Fig. 3F-J**), and an increase in the number of the striatal iNOS+ cells of rats exposed to ethanol ($^{\#}P$<0.05) (**Fig. 3P-T**).

3.10. Effect of OEA and AEA on cell damage and apoptosis in the striatum of ethanol-exposed rats

Alcohol consumption in diet induced an increase in the number of immunoreactive cells for the cell damage marker FosB and the cell apoptotic factor cleaved caspase 3 (**P<0.01) (**Fig. 4A,F**). Regarding treatment during alcoholic diet, no changes were found in the number of FosB+ cells in the striatum of OEA and AEA-treated rats (**Fig. 4A-E**). We observed a significant increase in the number of cleaved caspase 3+ cells in the striatum of the rats treated with OEA compared to those of ethanol-vehicle group ($^{\#}P$<0.05) (**Fig. 4F-J**).

3.11. Effect of OEA and AEA on apoptotic phenotyping of glial cells in the striatum of ethanol-exposed rats

We evaluated the number of astroglial and microglial cells expressing the apoptotic factor cleaved caspase 3 (**Fig. 5**). Our results showed that ethanol consumption induced a decrease in the number of cleaved caspase 3+ cells expressing Iba-1 (**P<0.01), but not GFAP, in the striatum (**Fig. 5A-F**). Curiously, we found a reduction in the number of GFAP+/cleaved caspase 3+ cells in the striatum of ethanol-exposed rats treated with OEA ($^{\#}P$<0.05) (**Fig. 5A-**

E). No effects of OEA and AEA were observed on the number of Iba-1+/cleaved caspase 3+ cells (**Fig. 5F-J**).

3.12. Effect of OEA and AEA on PPARα expression in the striatum of ethanol-exposed rats

As a high number of striatal neurons express PPARα, the main OEA receptor, we evaluated whether OEA and AEA can affect the presence and survival of PPARα+ cells as well as their putative expression in microglial cells. Ethanol consumption in diet induced an increase in the number of striatal PPARα+ cells (**Fig. 6A-C**) and a reduction in the number of PPARα+ cells expressing the apoptotic factor cleaved caspase 3 (*/***P<0.05/0.001) (**Fig. 6F-H**). Both OEA and AEA completely counteracted the ethanol effect on the number of PPARα+ cells ($^{\#\#\#}P$<0.001) (**Fig. 6A-E**), but not on PPARα+ cell survival (**Fig. 6F-J**) or PPARα+ cells expressing Iba-1 (**Fig. 6K-O**).

3.13. Effect of OEA and AEA on cell proliferation in the subventricular zone of ethanol-exposed rats

The subventricular zone (SVZ) of the lateral ventricles is a relevant neurogenic niche of the adult striatum. We evaluated the number of newborn cells in the SVZ by the analysis of the mitosis-related protein phospho (Ser-10)-histone H3 and after the administration of BrdU (50 mg/kg) for 4 days (**Fig. 7**). Phosphorylation at the residue Ser-10 in the histone H3 is considered a crucial event for the onset of mitosis. BrdU, a synthetic nucleoside that is an analog of thymidine, can be incorporated into the newly synthesized DNA of replicating cells. The number of phospho-H3+ cells and BrdU+ cells were decreased in the SVZ of rats exposed to ethanol (*P<0.05) (**Fig. 7A-J**). Interestingly, OEA counteracted the deleterious effect of ethanol as it specifically increased the number of phospho-H3+ cells and BrdU+

cells in the SVZ of rats exposed to ethanol ($^{\#\#}P<0.01$) (**Fig. 7A-J**). No effects of AEA on cell proliferation in SVZ were found.

3.14. Effect of OEA and AEA on cell phenotyping of the newborn cells in the SVZ of ethanol-exposed rats

To phenotype the newborn cells in the SVZ, we evaluated the number of BrdU+ cells showing a precursor (GFAP) or mature (β3-tubulin) neuronal, or microglial (Iba-1) phenotype. No significant changes were observed in the number of BrdU+ cells expressing GFAP in rats exposed to ethanol (**Fig. 8A-E**). However, rats exposed to alcoholic diet showed a lower number of BrdU+ cells expressing β3-tubulin ($^{*}P<0.05$) (**Fig. 8F-J**) and Iba-1 ($^{***}P<0.001$) (**Fig. 8K-O**) compared to those of the sucrose group. Both OEA and AEA specifically induced an increase in the number of BrdU+ cells expressing β3-tubulin that counteracted the deleterious effect of ethanol ($^{\#/\#\#}P<0.05/0.01$) (**Fig. 8F**).

4. DISCUSSION

PPARα agonists are anti-inflammatory, neuroprotective and have anti-addictive properties (Anton et al., 2016; Bilbao et al., 2016). Particularly, recent evidence suggests that drugs targeting PPARα can be effective in treating alcohol dependence among other addictions (Plaza-Zabala et al., 2010; Le Foll et al., 2013; Ferguson et al., 2014; Bilbao et al., 2013, 2016). Bilbao and collaborators (2016) demonstrated an enhancement of OEA mobilization in the nucleus accumbens after ethanol administration, which in turn reduced alcohol consumption by activating PPARα. In addition, a decrease in OEA levels was associated with alcohol withdrawal symptoms. The acute i.p. administration of OEA (5 mg/kg) confirmed the reduction of alcohol intake and self-administration, and blocked cue-induced reinstatement of alcohol-seeking behavior and somatic withdrawal symptoms after cessation of alcohol

consumption (Bilbao et al., 2016). These results suggested that OEA acts as an endogenous signal that modulates the homeostatic adaption of alcohol, including multiple physiological aspects and behavioral symptoms associated with motivation that extend to the control of contextual memories. In our rat model of daily exposure of ethanol added in diet (10%) for 2 weeks, the repeated administration of OEA (10 mg/kg) for the last 5 days of ethanol exposure didn't increased ethanol intake, as was observed for AEA and ACEA (present study; Rivera et al., 2015b). Interestingly, we found that OEA, as well as AEA, increased the ethanol-induced hypolocomotion. A previous study also described that the pharmacological administration of the synthetic PPARα activator fenofibrate after weaning during ethanol withdrawal modified the perturbed locomotor behavior observed in a rat model of early alcohol exposure (Marche et al., 2011). It should be noted that PPARα is highly expressed in tyrosine-hydroxylase positive neurons and related structures like the striatum (Galán-Rodríguez et al., 2009; Plaza-Zabala et al., 2010). Moreover, both PPARα agonists fenofibrate and tesaglitazar modified the gene expression profiling of the amygdala and prefrontal cortex, two important brain areas for reward and dependence directly related with striatum (Ferguson et al., 2014). In this regard, several data (present study; Bilbao et al., 2016) suggest that alcohol effects appear to rely on specific mechanisms related to PPARα signaling in the basal ganglia as alcohol increased the OEA levels, the gene expression of OEA-synthesizing enzyme *Nape-pld*, the number of PPARα-immunoreactive neurons and damage cell activity (FosB) in the striatum.

OEA also plays a central role in the regulation of cell survival and neuroprotection as it is synthesized on demand by local stimuli that accumulates in the brain after neurotoxic insults related to cellular stress and tissue damage (Walter et al., 2002; Schäbitz et al., 2002; Ouk et al., 2014). PPAR activity in brain is relatively high and PPARα is expressed in astrocytes, microglia and oligodendrocytes (Heneka and Landreth, 2007). In agreement with these findings, fenofibrate is able to enhance vasculoprotection and anti-inflammatory mechanisms

to protect against brain ischemia (Ouk et al., 2014), as well as to inhibit hippocampal microglial activation in whole-brain irradiation (Ramanan et al., 2009). Alcohol-induced brain damage likely impacts the function of resident immune cells of the central nervous system, particularly the cytokine production by astrocytes and microglia (Barr et al., 2016). There is also evidence of long-lasting consequences of hippocampal microglial activation caused by binge alcohol exposure during adolescence (McClain et al., 2011). Ethanol-induced microglia activation and neuronal apoptosis is modulated by the innate immunity TLR4 signaling pathway and enhances NF-kB-related inflammatory mediators (Fernández-Lizarbe et al., 2009, 2013; Alfonso-Loeches and Guerri, 2011; Crews et al., 2013). Interestingly, a recent study reported that OEA blocked several neuroimmune danger signaling pathways induced by ethanol binge administration such as HMGB1, TLR4 and the NF-kB proinflammatory cascades in the rat frontal cortex (Anton et al., 2016). Regarding the present study, OEA treatment during prolonged ethanol exposure modulates resident neuroimmune cells in the striatum as it increased the number of activated microglia (Iba-1+ cells and iNOS+ cells) and reduced the activated astroglia (vimentin immunoreactivity) (**Fig. 9A**). Despite previous studies suggesting the lack of induction of apoptosis by OEA, compared to AEA, in human neuroblastoma cells (Maccarrone and Finazzi-Agró, 2003), recent data demonstrated that OEA dose-dependently increased cell cytotoxicity and favored a decrease in cell viability in murine N1E-115 neuroblastoma cells (Hamtiaux et al., 2011). Our results clearly indicated an enhancement of apoptosis, as OEA increased ethanol-induced apoptosis (cleaved caspase 3+ cells) in the rat striatum. It has been documented that chronic microglial activation may contribute to an incorrect response to neuronal injury by removing damaged cells via phagocytosis (Dheen et al., 2007), an effect that could be enhanced by OEA-PPARα interaction in an alcoholic environment. Further studies are needed to elucidate whether the converging actions between ethanol and PPARα activation in the striatum produce an increase

475 in neuronal cell death (associated with ROS and TNFα; Alfonso-Loeches and Guerri, 2011;
476 Guadagno et al., 2013) or a malfunctioning of microglial activity (neurotoxic substances don´t
477 amplify the immune TLR4 responses) resulting in a decrease in phagocytic activity as was
478 previously described by AEA and PEA after focal cerebral ischemia (Franklin et al., 2003).
479 Varying consequences of adult neurogenesis result from the regulation of proliferation,
480 differentiation and survival of neural stem/progenitor cells (NSPCs) by addictive drugs.
481 Alcohol inhibits NSPC proliferation in adult rats exposed to acute and chronic alcohol binge
482 underlying cognitive dysfunction (Geil et al., 2014). However, survival of new-born NSPCs
483 in the dentate gyrus was impaired 28 days after chronic but not acute alcohol exposure, an
484 effect that was likely associated with cell apoptosis (Nixon and Crews, 2002; Herrera et al.,
485 2003). Chronic alcohol exposure was accompanied by an inhibition of neuronal
486 differentiation (decreased number of immature doublecortin+ cells) and neuronal survival of
487 new-born NSPCs (reduced number of cells co-labeled with both BrdU and the neuron-specific
488 marker NeuN) (He et al., 2005; Contet et al., 2014). Converging actions exist between forced
489 alcohol binge and cannabinoid receptor activation by WIN55,212-2 (2 mg/kg) for 5 days
490 resulting in reduced NSPC proliferation (Alen et al., 2010). In contrast, a recent study from
491 our group highlighted that the selective CB2 receptor agonist JWH133 specifically
492 counteracted the chronic ethanol exposure-induced impairment of NSPC proliferation and
493 maturation in the main neurogenic niches of the adult rat brain (Rivera et al., 2015b). PPAR
494 isoforms can directly regulate neuronal cell proliferation, survival and differentiation (Cimini
495 and Ceru, 2008; Di Giacomo et al., 2017). Specifically, PPARα can be implicated in the
496 progressive age-associated decline of NSPC proliferation (2, 6 and 18 months), an effect that
497 was partially compensated in enriched environments when PPARα is lacking (Pérez-Martín et
498 al., 2016). The present study goes further in the potential role of PPARα in other
499 neurodegenerative challenges like alcohol exposure in which a loss of neurons is described.

Thus, the PPARα agonist OEA counteracted the deleterious effect of ethanol on NSPC proliferation (phospho-H3 and BrdU) and neuronal maturation (β3-tubulin+/BrdU+) in the SVZ (**Fig. 9B**). Beside neurogenesis and activation of resting microglial, the present study also probed the concept of microgliogenesis in adult brain, a critical response in pathological conditions that has not been fully explored (Barua et al., 2017). We found a reduction in the number of new-born cells expressing Iba-1 (Iba1+/BrdU+ cells) in the SVZ of alcohol-exposed rats that was not affected after OEA treatment.

Overall, the findings presented here add to the previous described roles of the PPARα agonist OEA, including the lack of alcohol intake increase and the enhancement of ethanol-induced hypolocomotion when it was administered during ethanol exposure. OEA is an active signaling player in the activity of resident immune cells (astrocytes and microglia) affecting cell apoptosis, which are likely influenced by the impaired effects of ethanol on striatal PPARα+ cell population. The regulatory effects of OEA on NSPC proliferation and neuronal maturation in a context of alcohol exposure extend previous evidence suggesting a potential role of the PPARα signaling system in response to alcohol-specific behavioral and neurodegenerative alterations.

5. AUTHOR CONTRIBUTIONS

The authors have declared that no competing interest exists. All authors had full access to all the data in the study and take responsibility for the integrity of the data and the accuracy of the data analysis. PR, FRF and JS were responsible for the study concept and design. PR, DS, EB, AV, SA and LB contributed to the acquisition of data. LB performed the LC-MRM analysis. PR, AS, FJP, FRF and JS assisted with data analysis and interpretation of findings. FRF and JS drafted of the manuscript. BL, FRF and JS provided critical revision of the

manuscript for important intellectual content, obtained funding and study supervision. All authors approved final version for publication.

6. FUNDING

This work was supported by Instituto de Salud Carlos III (ISCIII), Ministerio de Economía y Competitividad (MINECO) co-funded by UE-ERDF program (JS: PI16/01374; FRF: PI16/01698); Ministerio de Sanidad, Servicios Sociales e Igualdad and Plan Nacional sobre Drogas (JS: PNSD2015/047); Consejería de Economía, Innovación y Ciencia, Junta de Andalucía, UE-ERDF (FRF: CTS-8221); Consejería de Salud, Junta de Andalucía, UE-ERDF (FRF: SAS111224; PR: PI-0337-2012); German Research Foundation DFG (BL: FOR926, project CP1). FJP (CP14/00212) and AS (CP14/00173) are recipients of a research contract from "Miguel Servet" Program of ISCIII, EU-ERDF. JS holds a "Miguel Servet II" research contract from the National System of Health, ISCIII, EU-ERDF, FIMABIS (CPII17/00024). PR holds a "Sara Borrel" research contract from ISCIII, EU-ERDF (CD16/00067).

7. REFERENCE

Aguado T, Monory K, Palazuelos J, Stella N, Cravatt B, Lutz B, Marsicano G, Kokaia Z, Guzmán M, Galve-Roperh I. 2005. The endocannabinoid system drives neural progenitor proliferation. FASEB J 19:1704-6.

Alén F, Mouret A, Viveros MP, Llorente R, Lepousez G, Lledo PM, López-Moreno JA. Converging action of alcohol consumption and cannabinoid receptor activation on adult hippocampal neurogenesis. Int J Neuropsychopharmacol. 2010 Mar;13(2):191-205. doi: 10.1017/S1461145709991118.

Alfonso-Loeches S, Guerri C. Molecular and behavioral aspects of the actions of alcohol on the adult and developing brain. Crit Rev Clin Lab Sci. 2011 Jan-Feb;48(1):19-47. doi: 10.3109/10408363.2011.580567.

Antón M, Alén F, Gómez de Heras R, Serrano A, Pavón FJ, Leza JC, García-Bueno B, Rodríguez de Fonseca F, Orio L. Oleoylethanolamide prevents neuroimmune HMGB1/TLR4/NF-kB danger signaling in rat frontal cortex and depressive-like behavior induced by ethanol binge administration. Addict Biol. 2017 May;22(3):724-741. doi: 10.1111/adb.12365.

Bandiera T, Ponzano S, Piomelli D. 2014. Advances in the discovery of N-acylethanolamine acid amidase inhibitors. Pharmacol Res 86:11-7. doi:10.1016/j.phrs.2014.04.011.

Barr T, Helms C, Grant K, Messaoudi I. Opposing effects of alcohol on the immune system. Prog Neuropsychopharmacol Biol Psychiatry. 2016 Feb 4;65:242-51. doi: 10.1016/j.pnpbp.2015.09.001.

Barson JR, Karatayev O, Chang GQ, Johnson DF, Bocarsly ME, Hoebel BG, Leibowitz SF. Positive relationship between dietary fat, ethanol intake, triglycerides, and hypothalamic peptides: counteraction by lipid-lowering drugs. Alcohol. 2009 Sep;43(6):433-41. doi: 10.1016/j.alcohol.2009.07.003.

Barua S, Chung JI, Kim AY, Lee SY, Lee SH, Baik EJ. Jak kinase 3 signaling in microgliogenesis from the spinal nestin+ progenitors in both development and response to injury. Neuroreport. 2017 Sep 27;28(14):929-935. doi:10.1097/WNR.0000000000000854.

Bilbao A, Blanco E, Luque-Rojas MJ, Suárez J, Palomino A, Vida M, Araos P, Bermúdez-Silva FJ, Fernández-Espejo E, Spanagel R, Rodríguez de Fonseca F. Oleoylethanolamide dose-dependently attenuates cocaine-induced behaviours through a PPARα receptor-independent mechanism. Addict Biol. 2013 Jan;18(1):78-87. doi:10.1111/adb.12006.

Bilbao A, Serrano A, Cippitelli A, Pavón FJ, Giuffrida A, Suárez J, García-Marchena N, Baixeras E, Gómez de Heras R, Orio L, Alén F, Ciccocioppo R, Cravatt BF, Parsons LH, Piomelli D, Rodríguez de Fonseca F. Role of the satiety factor oleoylethanolamide in alcoholism. Addict Biol. 2016 Jul;21(4):859-72. doi:10.1111/adb.12276

Bindila L and Lutz B. Extraction and Simultaneous Quantification of Endocannabinoids and Endocannabinoid-Like Lipids in Biological Tissues. Methods in Molecular Biology, 2016; 1412:9-18

Campolongo P, Roozendaal B, Trezza V, Cuomo V, Astarita G, Fu J, McGaugh JL, Piomelli D. Fat-induced satiety factor oleoylethanolamide enhances memory consolidation. Proc Natl Acad Sci U S A. 2009 May 12;106(19):8027-31. doi:10.1073/pnas.0903038106.

Cimini A, Cerù MP. Emerging roles of peroxisome proliferator-activated receptors (PPARs) in the regulation of neural stem cells proliferation and differentiation. Stem Cell Rev. 2008 Dec;4(4):293-303. doi:10.1007/s12015-008-9024-2.

Cippitelli A, Cannella N, Braconi S, Duranti A, Tontini A, Bilbao A, De Fonseca FR, Piomelli D, Ciccocioppo R. 2008. Increase of brain endocannabinoid anandamide levels by FAAH inhibition and alcohol abuse behaviours in the rat. Psychopharmacology (Berl) 198:449-60. doi: 10.1007/s00213-008-1104-0.

Colombo G, Serra S, Vacca G, Carai MA, Gessa GL. 2005. Endocannabinoid system and alcohol addiction: pharmacological studies. Pharmacol Biochem Behav 81:369-80.

Contet C, Kim A, Le D, Iyengar SK, Kotzebue RW, Yuan CJ, Kieffer BL, Mandyam CD. μ-Opioid receptors mediate the effects of chronic ethanol binge drinking on the hippocampal neurogenic niche. Addict Biol. 2014 Sep;19(5):770-80. doi:10.1111/adb.12040.

Crews FT, Qin L, Sheedy D, Vetreno RP, Zou J. High mobility group box 1/Toll-like receptor danger signaling increases brain neuroimmune activation in alcohol dependence. Biol Psychiatry. 2013 Apr 1;73(7):602-12. doi:10.1016/j.biopsych.2012.09.030.

Crews FT, Nixon K. 2009. Mechanisms of neurodegeneration and regeneration in alcoholism. Alcohol Alcohol 44:115-27. doi: 10.1093/alcalc/agn079.

Dheen ST, Kaur C, Ling EA. Microglial activation and its implications in the brain diseases. Curr Med Chem. 2007;14(11):1189-97.

Di Giacomo E, Benedetti E, Cristiano L, Antonosante A, d'Angelo M, Fidoamore A, Barone D, Moreno S, Ippoliti R, Cerù MP, Giordano A, Cimini A. Roles of PPAR transcription factors in the energetic metabolic switch occurring during adult neurogenesis. Cell Cycle. 2017 Jan 2;16(1):59-72. doi:10.1080/15384101.2016.1252881.

Di Marzo V. Endocannabinoid signaling in the brain: biosynthetic mechanisms in the limelight. Nat Neurosci. 2011 Jan;14(1):9-15. doi: 10.1038/nn.2720.

Ferguson LB, Most D, Blednov YA, Harris RA. PPAR agonists regulate brain gene expression: relationship to their effects on ethanol consumption. Neuropharmacology. 2014 Nov;86:397-407. doi: 10.1016/j.neuropharm.2014.06.024.

Fernandez-Lizarbe S, Montesinos J, Guerri C. Ethanol induces TLR4/TLR2 association, triggering an inflammatory response in microglial cells. J Neurochem. 2013 Jul;126(2):261-73. doi: 10.1111/jnc.12276.

Fernandez-Lizarbe S, Pascual M, Guerri C. Critical role of TLR4 response in the activation of microglia induced by ethanol. J Immunol. 2009 Oct 1;183(7):4733-44. doi: 10.4049/jimmunol.0803590.

Franklin A, Parmentier-Batteur S, Walter L, Greenberg DA, Stella N. Palmitoylethanolamide increases after focal cerebral ischemia and potentiates microglial cell motility. J Neurosci. 2003 Aug 27;23(21):7767-75.

Fowler CJ, Rojo ML, Rodriguez-Gaztelumendi A. 2010. Modulation of the endocannabinoid system: neuroprotection or neurotoxicity? Exp Neurol 224:37-47. doi: 10.1016/j.expneurol.2010.03.021

Fu J, Dipatrizio NV, Guijarro A, Schwartz GJ, Li X, Gaetani S, Astarita G, Piomelli D. Sympathetic activity controls fat-induced oleoylethanolamide signaling in small intestine. J Neurosci. 2011 Apr 13;31(15):5730-6. doi:10.1523/JNEUROSCI.5668-10.2011.

Galan-Rodriguez B, Suarez J, Gonzalez-Aparicio R, Bermudez-Silva FJ, Maldonado R, Robledo P, Rodriguez de Fonseca F, Fernandez-Espejo E. 2009. Oleoylethanolamide exerts partial and dose-dependent neuroprotection of substantia nigra dopamine neurons. Neuropharmacology 56:653-64. doi:10.1016/j.neuropharm.2008.11.006.

Galve-Roperh I, Chiurchiù V, Díaz-Alonso J, Bari M, Guzmán M, Maccarrone M. 2013. Cannabinoid receptor signaling in progenitor/stem cell proliferation and differentiation. Prog Lipid Res 52:633-50. doi:10.1016/j.plipres.2013.05.004.

Garcia-Marchena N, Pavon FJ, Pastor A, Araos P, Pedraz M, Romero-Sanchiz P, Calado M, Suarez J, Castilla-Ortega E, Orio L, Boronat A, Torrens M, Rubio G, de la Torre R, Rodriguez de Fonseca F, Serrano A. Plasma concentrations of oleoylethanolamide and other acylethanolamides are altered in alcohol-dependent patients: effect of length of abstinence. Addict Biol. 2017 Sep;22(5):1366-1377. doi: 10.1111/adb.12408.

Geil CR, Hayes DM, McClain JA, Liput DJ, Marshall SA, Chen KY, Nixon K. Alcohol and adult hippocampal neurogenesis: promiscuous drug, wanton effects. Prog Neuropsychopharmacol Biol Psychiatry. 2014 Oct 3;54:103-13. doi:10.1016/j.pnpbp.2014.05.003.

Goncalves MB, Suetterlin P, Yip P, Molina-Holgado F, Walker DJ, Oudin MJ, Zentar MP, Pollard S, Yáñez-Muñoz RJ, Williams G, Walsh FS, Pangalos MN, Doherty P. 2008. A diacylglycerol lipase-CB2 cannabinoid pathway regulates adult subventricular zone neurogenesis in an age-dependent manner. Mol Cell Neurosci 38:526-36.

Guadagno J, Xu X, Karajgikar M, Brown A, Cregan SP. Microglia-derived TNFα induces apoptosis in neural precursor cells via transcriptional activation of the Bcl-2 family member Puma. Cell Death Dis. 2013 Mar 14;4:e538. doi:10.1038/cddis.2013.59.

Guzmán M, Lo Verme J, Fu J, Oveisi F, Blázquez C, Piomelli D. Oleoylethanolamide stimulates lipolysis by activating the nuclear receptor peroxisome proliferator-activated receptor alpha (PPAR-alpha). J Biol Chem. 2004 Jul 2;279(27):27849-54.

Hamtiaux L, Hansoulle L, Dauguet N, Muccioli GG, Gallez B, Lambert DM. 2011. Increasing antiproliferative properties of endocannabinoids in N1E-115 neuroblastoma cells through inhibition of their metabolism. PLoS One 6:e26823. doi: 10.1371/journal.pone.0026823.

He DY, McGough NN, Ravindranathan A, Jeanblanc J, Logrip ML, Phamluong K, Janak PH, Ron D. Glial cell line-derived neurotrophic factor mediates the desirable actions of the anti-addiction drug ibogaine against alcohol consumption. J Neurosci. 2005 Jan 19;25(3):619-28.

Heneka MT, Landreth GE. PPARs in the brain. Biochim Biophys Acta. 2007 Aug;1771(8):1031-45.

Herrera DG, Yague AG, Johnsen-Soriano S, Bosch-Morell F, Collado-Morente L, Muriach M, Romero FJ, Garcia-Verdugo JM. 2003. Selective impairment of hippocampal neurogenesis by chronic alcoholism: protective effects of an antioxidant. Proc Natl Acad Sci U S A 100:7919-24.

Katona I, Freund TF. 2012. Multiple functions of endocannabinoid signaling in the brain. Annu Rev Neurosci 35:529-58. doi:10.1146/annurev-neuro-062111-150420.

Le Foll B, Di Ciano P, Panlilio LV, Goldberg SR, Ciccocioppo R. Peroxisome proliferator-activated receptor (PPAR) agonists as promising new medications for drug addiction: preclinical evidence. Curr Drug Targets. 2013 Jun;14(7):768-76.

Lomazzo E, Bindila L, Remmers F, Lerner R, Schwitter C, Hoheisel U, Lutz B. 2014. Therapeutic potential of inhibitors of endocannabinoid degradation for the treatment of stress-related hyperalgesia in an animal model of chronic pain. Neuropsychopharmacology. Aug 6. doi: 10.1038/npp.2014.198.

LoVerme J, Guzmán M, Gaetani S, Piomelli D. Cold exposure stimulates synthesis of the bioactive lipid oleoylethanolamide in rat adipose tissue. J Biol Chem. 2006 Aug 11;281(32):22815-8.

Maccarrone M, Finazzi-Agró A. 2003. The endocannabinoid system, anandamide and the regulation of mammalian cell apoptosis. Cell Death Differ 10:946-55.

Marche K, Danel T, Bordet R. Fetal alcohol-induced hyperactivity is reversed by treatment with the PPARα agonist fenofibrate in a rat model. Psychopharmacology (Berl). 2011 Mar;214(1):285-96. doi:10.1007/s00213-010-1960-2.

Mascia P, Pistis M, Justinova Z, Panlilio LV, Luchicchi A, Lecca S, Scherma M, Fratta W, Fadda P, Barnes C, Redhi GH, Yasar S, Le Foll B, Tanda G, Piomelli D, Goldberg SR. Blockade of nicotine reward and reinstatement by activation of alpha-type peroxisome proliferator-activated receptors. Biol Psychiatry. 2011 Apr 1;69(7):633-41. doi: 10.1016/j.biopsych.2010.07.009.

McClain JA, Morris SA, Deeny MA, Marshall SA, Hayes DM, Kiser ZM, Nixon K. Adolescent binge alcohol exposure induces long-lasting partial activation of microglia. Brain Behav Immun. 2011 Jun;25 Suppl 1:S120-8. doi:10.1016/j.bbi.2011.01.006.

Nixon K, Crews FT. Binge ethanol exposure decreases neurogenesis in adult rat hippocampus. J Neurochem. 2002 Dec;83(5):1087-93.

Nixon K, Crews FT. 2004. Temporally specific burst in cell proliferation increases hippocampal neurogenesis in protracted abstinence from alcohol. J Neurosci 24:9714-22.

Orio L, Pavón FJ, Blanco E, Serrano A, Araos P, Pedraz M, Rivera P, Calado M, Suárez J, de Fonseca FR. Lipid transmitter signaling as a new target for treatment of cocaine addiction: new roles for acylethanolamides and lysophosphatidic acid. Curr Pharm Des. 2013;19(40):7036-49.

Ouk T, Gautier S, Pétrault M, Montaigne D, Maréchal X, Masse I, Devedjian JC, Deplanque D, Bastide M, Nevière R, Duriez P, Staels B, Pasquier F, Leys D, Bordet R. Effects of the PPAR-α agonist fenofibrate on acute and short-term consequences of brain ischemia. J Cereb Blood Flow Metab. 2014 Mar;34(3):542-51. doi:10.1038/jcbfm.2013.233.

Overton HA, Babbs AJ, Doel SM, Fyfe MC, Gardner LS, Griffin G, Jackson HC, Procter MJ, Rasamison CM, Tang-Christensen M, Widdowson PS, Williams GM, Reynet C. 2006 Deorphanization of a G protein-coupled receptor for oleoylethanolamide and its use in the discovery of small-molecule hypophagic agents. Cell Metab. 3: 167-75.

Paxinos G and Watson C. 2007. The rat brain in stereotaxic coordinates. Sidney: Academic Press. Sixth edition.

Pérez-Martín M, Rivera P, Blanco E, Lorefice C, Decara J, Pavón FJ, Serrano A, Rodríguez de Fonseca F, Suárez J. Environmental enrichment, age, and PPARα interact to regulate proliferation in neurogenic niches. Front Neurosci. 2016 Mar 9;10:89. doi: 10.3389/fnins.2016.00089.

Pertwee RG. 2008. Ligands that target cannabinoid receptors in the brain: from THC to anandamide and beyond. Addict Biol 13:147-59.

Piomelli D. A fatty gut feeling. Trends Endocrinol Metab. 2013 Jul;24(7):332-41. doi: 10.1016/j.tem.2013.03.001.

Piomelli D, Tarzia G, Duranti A, Tontini A, Mor M, Compton TR, Dasse O, Monaghan EP, Parrott JA, Putman D. 2006. Pharmacological profile of the selective FAAH inhibitor KDS-4103 (URB597). CNS Drug Rev 12:21-38.

Plaza-Zabala A, Berrendero F, Suarez J, Bermudez-Silva FJ, Fernandez-Espejo E, Serrano A, Pavon FJ, Parsons LH, De Fonseca FR, Maldonado R, Robledo P. Effects of the endogenous PPAR-alpha agonist, oleoylethanolamide on MDMA-induced cognitive deficits in mice. Synapse. 2010 May;64(5):379-89. doi:10.1002/syn.20733.

Ramanan S, Kooshki M, Zhao W, Hsu FC, Riddle DR, Robbins ME. The PPARalpha agonist fenofibrate preserves hippocampal neurogenesis and inhibits microglial activation after whole-brain irradiation. Int J Radiat Oncol Biol Phys. 2009 Nov 1;75(3):870-7. doi: 10.1016/j.ijrobp.2009.06.059.

Rivera P, Arrabal S, Vargas A, Blanco E, Serrano A, Pavón FJ, Rodríguez de Fonseca F, Suárez J. Localization of peroxisome proliferator-activated receptor alpha (PPARα) and N-acyl phosphatidylethanolamine phospholipase D (NAPE-PLD) in cells expressing the Ca(2+)-binding proteins calbindin, calretinin, and parvalbumin in the adult rat hippocampus. Front Neuroanat. 2014 Mar 17;8:12. doi:10.3389/fnana.2014.00012.

Rivera P, Bindila L, Pastor A, Pérez-Martín M, Pavón FJ, Serrano A, de la Torre R, Lutz B, Rodríguez de Fonseca F, Suárez J. Pharmacological blockade of the fatty acid amide hydrolase (FAAH) alters neural proliferation, apoptosis and gliosis in the rat hippocampus, hypothalamus and striatum in a negative energy context. Front Cell Neurosci. 2015 Mar 27;9:98. doi: 10.3389/fncel.2015.00098.

Rivera P, Blanco E, Bindila L, Alen F, Vargas A, Rubio L, Pavón FJ, Serrano A, Lutz B, Rodríguez de Fonseca F, Suárez J. Pharmacological activation of CB2 receptors counteracts the deleterious effect of ethanol on cell proliferation in the main neurogenic zones of the adult rat brain. Front Cell Neurosci. 2015 Sep 29;9:379. doi: 10.3389/fncel.2015.00379.

Rivera P, Pérez-Martín M, Pavón FJ, Serrano A, Crespillo A, Cifuentes M, López-Ávalos MD, Grondona JM, Vida M, Fernández-Llebrez P, de Fonseca FR, Suárez J. Pharmacological administration of the isoflavone daidzein enhances cell proliferation

764 and reduces high fat diet-induced apoptosis and gliosis in the rat hippocampus. PLoS
765 One. 2013 May 31;8(5):e64750. doi:10.1371/journal.pone.0064750.
766 Schäbitz WR, Giuffrida A, Berger C, Aschoff A, Schwaninger M, Schwab S, Piomelli D.
767 Release of fatty acid amides in a patient with hemispheric stroke: a microdialysis
768 study. Stroke. 2002 Aug;33(8):2112-4.
769 Serrano A, Pavón FJ, Tovar S, Casanueva F, Señarís R, Diéguez C, de Fonseca FR.
770 Oleoylethanolamide: effects on hypothalamic transmitters and gut peptides regulating
771 food intake. Neuropharmacology. 2011 Mar;60(4):593-601. doi:
772 10.1016/j.neuropharm.2010.12.007.
773 Serrano A, Rivera P, Pavón FJ, Decara J, Suárez J, Rodríguez de Fonseca F, Parsons LH.
774 2012. Differential effects of single versus repeated alcohol withdrawal on the
775 expression of endocannabinoid system-related genes in the rat amygdala. Alcohol Clin
776 Exp Res 36:984-994. doi: 10.1111/j.1530-0277.2011.01686.x.
777 Sipe JC, Chiang K, Gerber AL, Beutler E, Cravatt BF. A missense mutation in human fatty
778 acid amide hydrolase associated with problem drug use. Proc Natl Acad Sci U S A.
779 2002 Jun 11;99(12):8394-9.
780 Spanagel R. Alcoholism: a systems approach from molecular physiology to addictive
781 behavior. Physiol Rev. 2009 Apr;89(2):649-705. doi:10.1152/physrev.00013.2008.
782 Stella N. 2010. Cannabinoid and cannabinoid-like receptors in microglia, astrocytes, and
783 astrocytomas. Glia 58:1017-30. doi: 10.1002/glia.20983.
784 Stella N, Piomelli D. Receptor-dependent formation of endogenous cannabinoids in cortical
785 neurons. Eur J Pharmacol. 2001 Aug 17;425(3):189-96.
786 Suárez J, Rivera P, Arrabal S, Crespillo A, Serrano A, Baixeras E, Pavón FJ, Cifuentes M,
787 Nogueiras R, Ballesteros J, Dieguez C, Rodríguez de Fonseca F. Oleoylethanolamide
788 enhances β-adrenergic-mediated thermogenesis and white-to-brown adipocyte
789 phenotype in epididymal white adipose tissue in rat. Dis Model Mech. 2014
790 Jan;7(1):129-41. doi: 10.1242/dmm.013110.
791 Tellez LA, Medina S, Han W, Ferreira JG, Licona-Limón P, Ren X, Lam TT, Schwartz GJ,
792 de Araujo IE. A gut lipid messenger links excess dietary fat to dopamine deficiency.
793 Science. 2013 Aug 16;341(6147):800-2. doi:10.1126/science.1239275.
794 Ueda N, Tsuboi K, Uyama T. 2010. Enzymological studies on the biosynthesis of N-
795 acylethanolamines. Biochim Biophys Acta 1801:1274-85.
796 Walter L, Franklin A, Witting A, Moller T, Stella N. Astrocytes in culture produce
797 anandamide and other acylethanolamides. J Biol Chem. 2002 Jun 7;277(23):20869-76.

798

799

800

801

802

803

8. LEGENDS TO FIGURES

Figure 1. Experimental design of chronic ethanol exposure (10%) for 2 weeks (**A**) in order to evaluate ethanol consumption (**B**), distance covered in the open field (OF) (**C**), blood ethanol concentration (BEC), plasma levels of the hepatic enzymes gamma-glutamyl transpeptidase (γGT), glutamate pyruvate transaminase (GPT) and glutamic oxaloacetic transaminase (GOT) (**D**), plasma (**D**) and brain (**E**) levels of the endocannabinoids oleoylethanolamide (OEA) and anandamide (AEA), and mRNA levels of *Cnr1*, *Pparα*, *Nape-pld* and *Faah* in the striatum (**F**). The histograms represent the mean + s.e.m. (n=6) per experimental group. Bonferroni's or Student's *t* test: */**/***P<0.05/0.01/0.001 *vs*. sucrose diet-per fed group.

Figure 2. Experimental design of OEA and AEA i.p. administration (10 mg/kg) during the last 5 days of chronic ethanol exposure (10%) for 2 weeks (**A**) in order to evaluate sucrose (**B**) and ethanol (**C**) consumption, total distance covered in OF (**D**), distance covered in time bins of 5 minutes (**E**, **F**), plasma levels of the hepatic γGT and the GPT/GOT ratio (**G**), and plasma levels of the endocannabinoids OEA and AEA (**H**). The histograms represent the mean + s.e.m. (n=6) per experimental group. Bonferroni's test: */**/***P<0.05/0.01/0.001 *vs*. vehicle-sucrose group; $^{\#/\#\#/\#\#\#}P$<0.05/0.01/0.001 *vs*. vehicle-ethanol group; $^{\$}P$<0.05 *vs*. OEA-sucrose group.

Figure 3. Effects of OEA and AEA i.p. administration (10 mg/kg) during the last 5 days of chronic ethanol exposure (10%) for 2 weeks on GFAP, vimentin, Iba-1 and iNOS immunohistochemistry in the striatum. The histograms represent the mean + s.e.m. per area (mm^2) (n=6) of the number of GFAP+ cells (**A**), vimentin immunoreactivity (**F**), the number of Iba-1+ cells (**K**) and the number of iNOS+ cells (**P**) per experimental group. Bonferroni's test: *P<0.05 *vs*. vehicle-sucrose group; $^{\#/\#\#/\#\#\#}P$<0.05/0.01/0.001 *vs*. vehicle-ethanol group.

Representative microphotographs showing low and high (insets) magnification views of the respective immunostaining (**B-E**, **G-J**, **L-O**, **Q-T**). Scale bars are included in each image. Str, striatum; lv, lateral ventricle.

Figure 4. Effects of OEA and AEA i.p. administration (10 mg/kg) during the last 5 days of chronic ethanol exposure (10%) for 2 weeks on FosB and cleaved caspase 3 immunohistochemistry in the striatum. The histograms represent the mean + s.e.m. per area (mm^2) (*n*=6) of the number of FosB+ cells (**A**) and cleaved caspase 3+ cells (**F**) per experimental group. Bonferroni's test: ***P*<0.01 *vs*. vehicle-sucrose group; $^{\#}P$<0.05 *vs*. vehicle-ethanol group. Representative microphotographs showing low and high (insets) magnification views of the respective immunostaining (**B-E**, **G-J**). Scale bars are included in each image. Str, striatum; lv, lateral ventricle.

Figure 5. Effects of OEA and AEA i.p. administration (10 mg/kg) during the last 5 days of chronic ethanol exposure (10%) for 2 weeks on the immunofluorescent co-expression of cleaved caspase 3, GFAP and Iba-1 in striatal cells. The histograms represent the mean + s.e.m. per area (mm^2) (*n*=6) of the number of GFAP+/cleaved caspase 3+ cells (**A**) and Iba1+/cleaved caspase 3+ cells (**F**) per experimental group. Bonferroni's test: ***P*<0.01 *vs*. vehicle-sucrose group; $^{\#}P$<0.05 *vs*. vehicle-ethanol group. High resolution confocal laser scanning photomicrographs showing the respective co-labeling (**B-E**, **G-J**). Arrowheads indicate cleaved caspase 3+ cells expressing GFAP or Iba1. Scale bars indicated 25 μm.

Figure 6. Effects of OEA and AEA i.p. administration (10 mg/kg) during the last 5 days of chronic ethanol exposure (10%) for 2 weeks on the immunofluorescent co-expression of PPARα, cleaved caspase 3 and Iba1 in striatal cells. The histograms represent the mean +

s.e.m. per area (mm^2) (n=6) of the number of PPARα+ cells (**A**), PPARα+/cleaved caspase 3+ cells (**F**) and PPARα+/Iba1+ cells (**K**) per experimental group. Bonferroni's test: */***P<0.05/0.001 *vs*. vehicle-sucrose group; $^{###}P$<0.001 *vs*. vehicle-ethanol group. High resolution confocal laser scanning photomicrographs showing the respective co-labeling (**B-E**, **G-J**, **L-O**). Arrows indicate PPARα+ cells expressing cleaved caspase 3 or Iba1. Scale bars indicated 25 μm.

Figure 7. Effects of OEA and AEA i.p. administration (10 mg/kg) during the last 5 days of chronic ethanol exposure (10%) for 2 weeks on phospho-histone H3 (Ser-10) and 5´-bromo-2´-deoxyuridine (BrdU) immunohistochemistry in the SVZ. The histograms represent the mean + s.e.m. per area (mm^2) (n=6) of the number of phospho-$H3^+$ cells (**A**) and BrdU+ cells (**F**) per experimental group. Bonferroni's test: *P<0.05 *vs*. vehicle-sucrose group; $^{##}P$<0.01 *vs*. vehicle-ethanol group. Representative microphotographs showing low and high (insets) magnification views of the respective immunostaining (**B-E**, **G-J**). Scale bars are included in each image. Str, striatum; lv, lateral ventricle.

Figure 8. Effects of OEA and AEA i.p. administration (10 mg/kg) during the last 5 days of chronic ethanol exposure (10%) for 2 weeks on the immunofluorescent co-labeling of BrdU, GFAP, β3-tubulin and Iba1 in cells of the SVZ. The histograms represent the mean + s.e.m. per area (mm^2) (n=6) of the number of GFAP+/BrdU+ cells (**A**), β3-tubulin+/BrdU+ cells (**F**) and Iba1+/BrdU+ cells (**K**). Bonferroni's test: */***P<0.05/0.001 *vs*. vehicle-sucrose group; $^{#/###}P$<0.05/0.01 *vs*. vehicle-ethanol group. High resolution confocal laser scanning photomicrographs showing the respective co-labeling **(B-E**, **G-J**, **L-O)**. Arrowheads indicate BrdU+ cells expressing GFAP, β3-tubulin or Iba1. Scale bars indicated 25 μm.

879 **Figure 9.** Schematic drawing that summarize the effects of ethanol and OEA on astroglial and
880 microglial activity (**A**), and NSPC proliferation and neuronal maturation (**B**).

Figure 1

Click here to download high resolution image

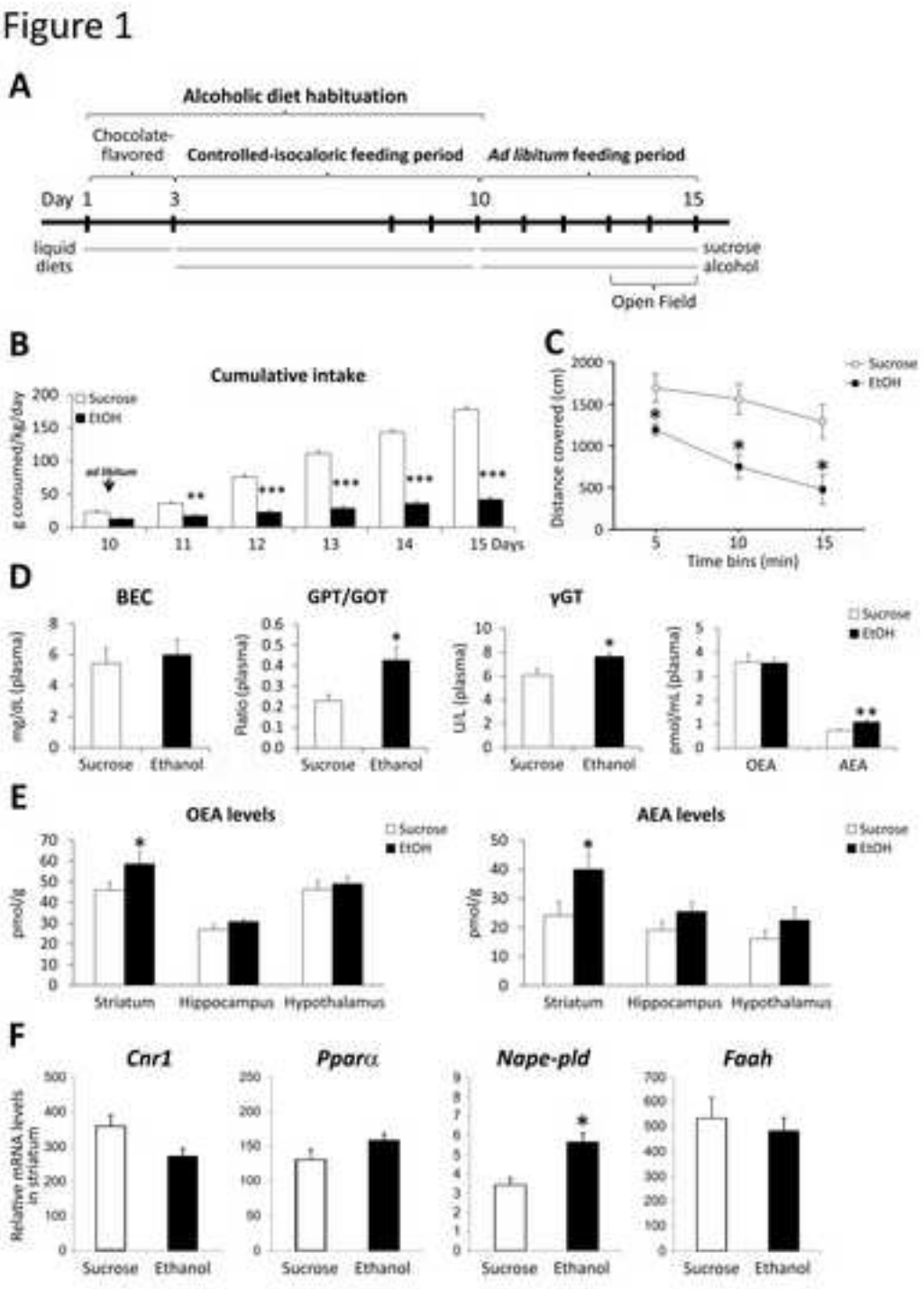

Figure 2

Click here to download high resolution image

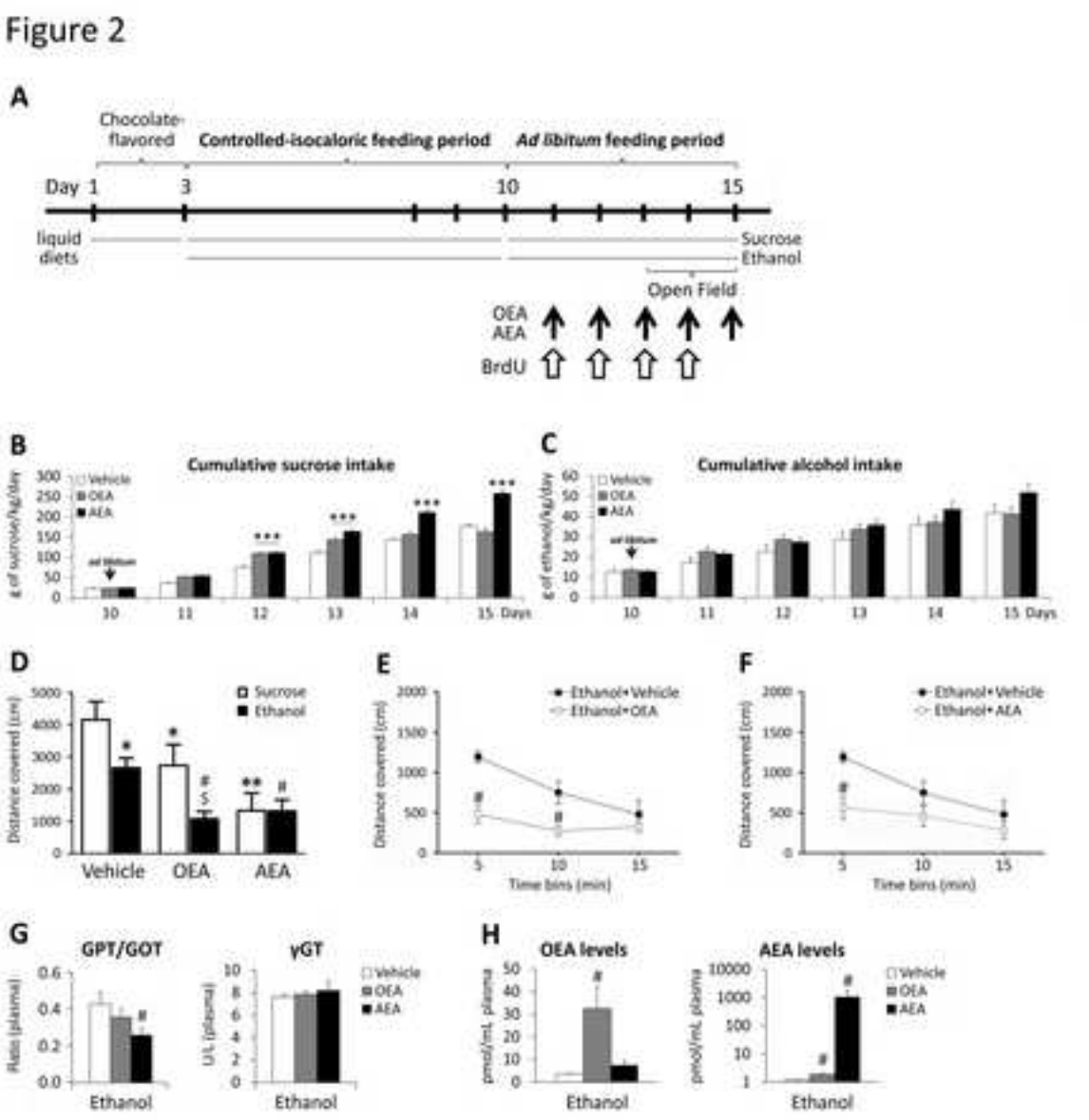

Figure 3

Click here to download high resolution image

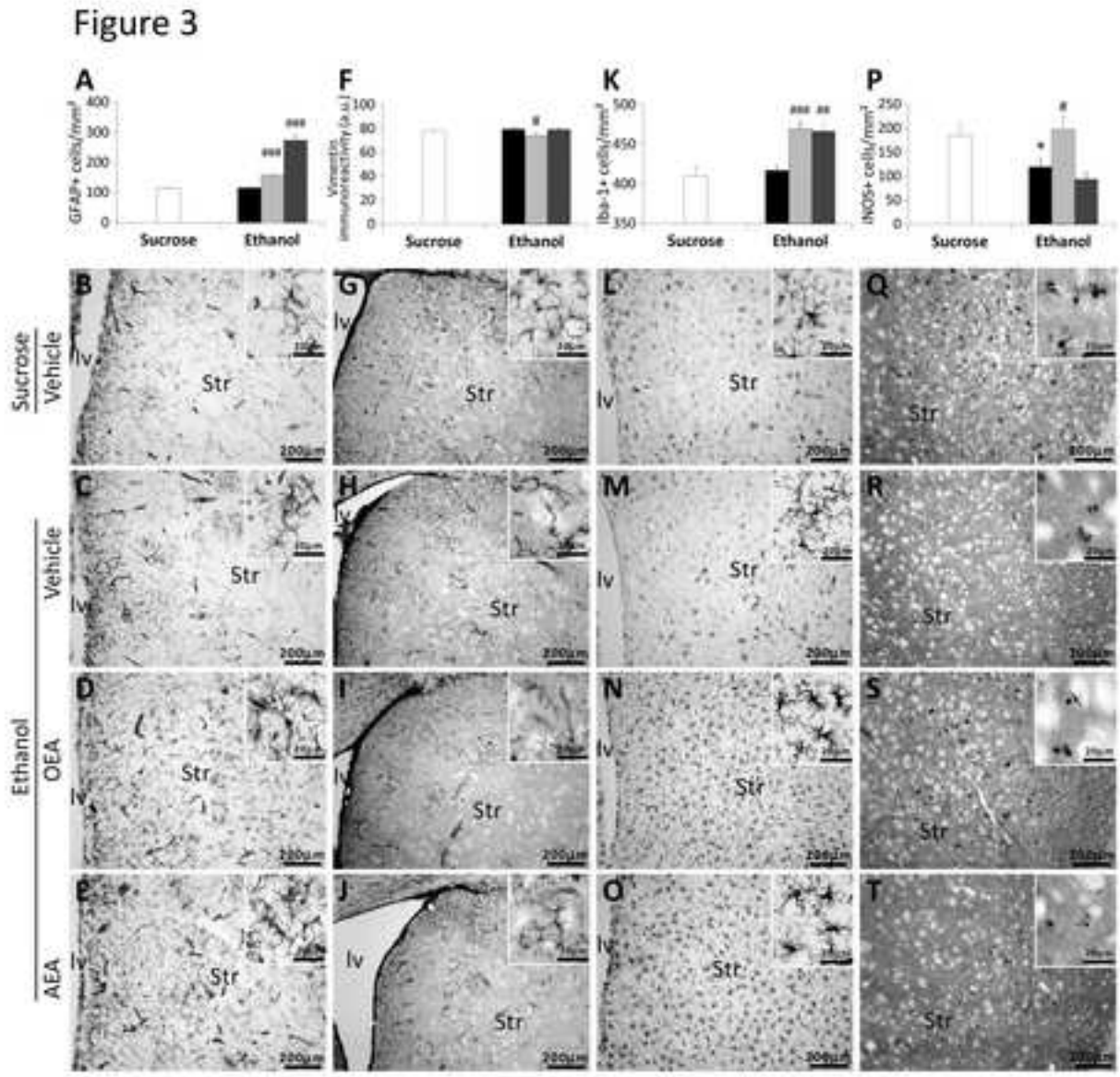

Figure 4

Click here to download high resolution image

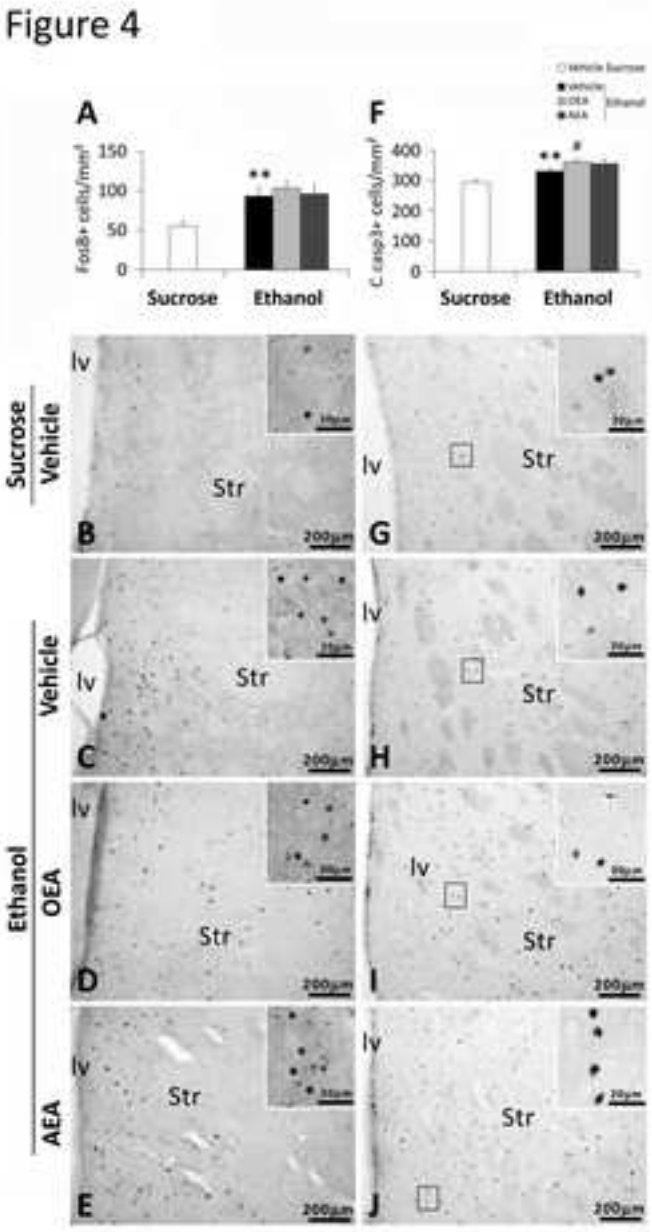

Figure 5

Click here to download high resolution image

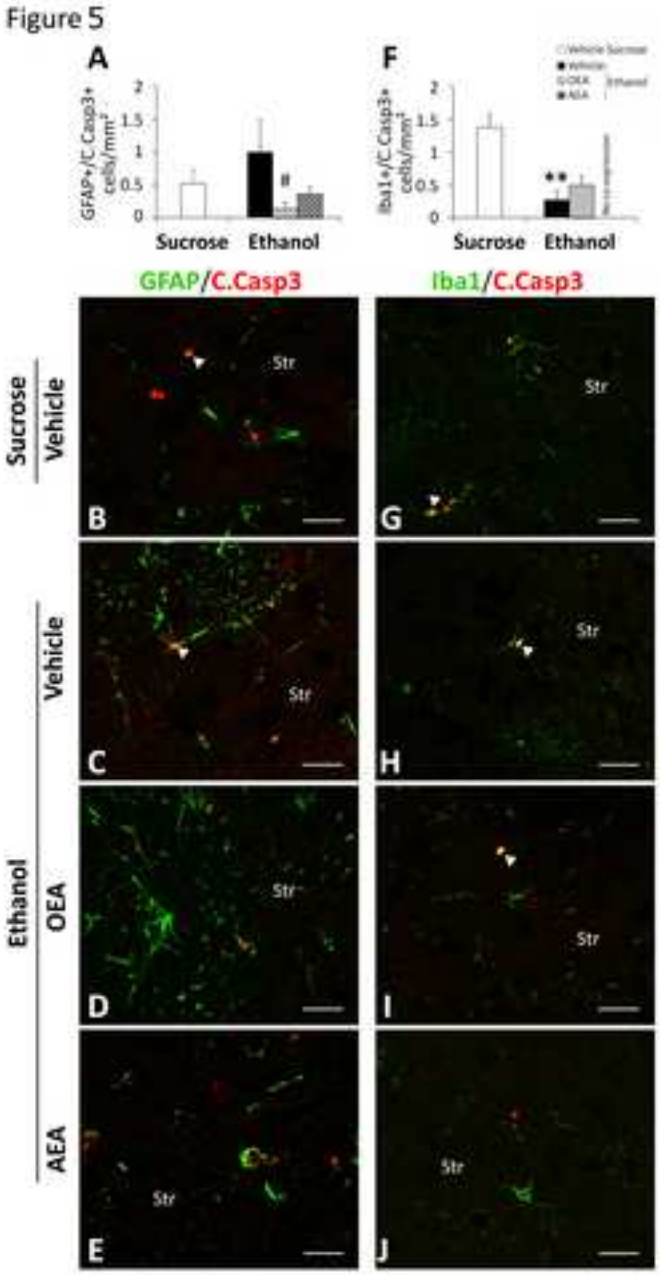

Figure 6

Click here to download high resolution image

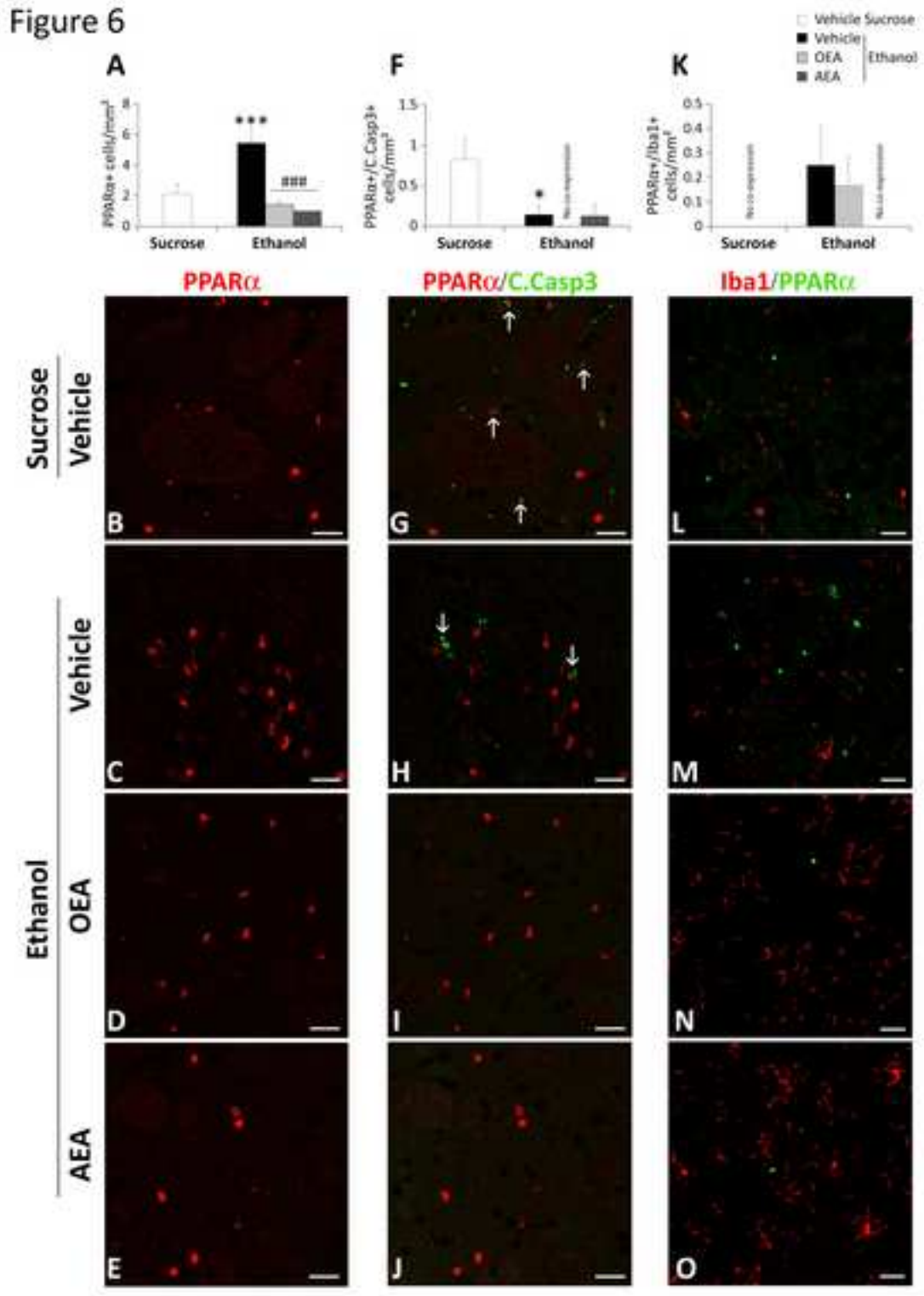

Figure 7

Click here to download high resolution image

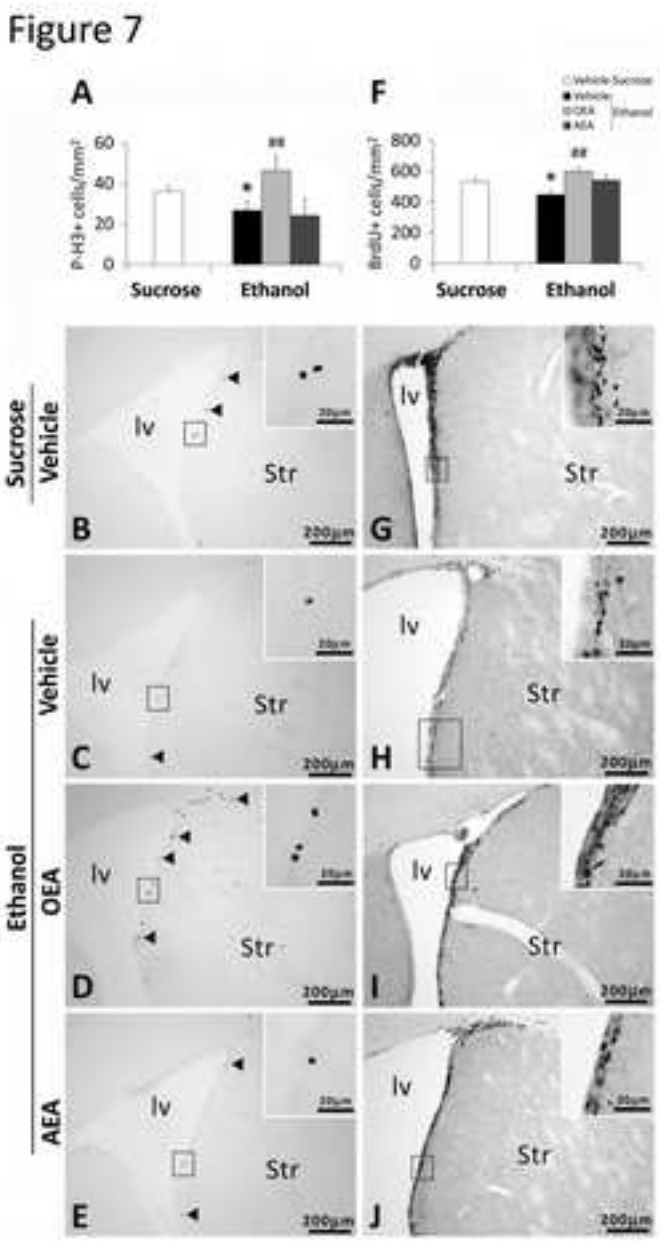

Figure 8

Click here to download high resolution image

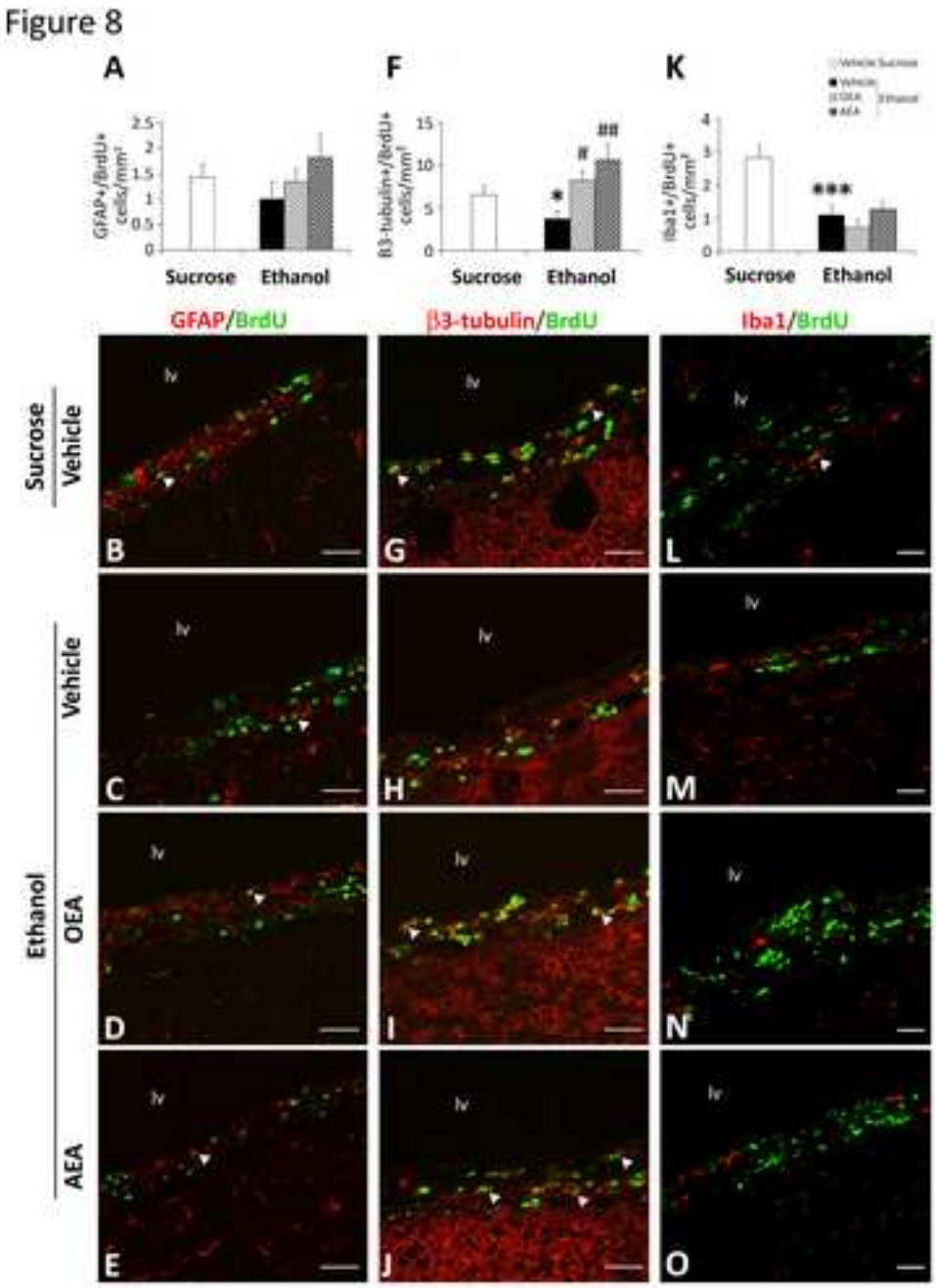

Figure 9

Click here to download high resolution image

Figure 9